Selective Oxidation of $[Rh^{I}(cod)]^{+}$ by H_2O_2 and O_2

Bas de Bruin,[a] Johanna A. Brands,[a] Jack J. J. M. Donners,[a] Maurice P. J. Donners,[a] René de Gelder,[a] Jan M. M. Smits,[a] Anton W. Gal,*[a] and Anton L. Spek[b]

Abstract: New, five-coordinate *Z*,*Z*-1,5-cyclooctadiene (cod) complexes $[{}'N_3'Rh^{I}(cod)]^{+}$ have been structurally characterised by NMR spectroscopy and X-ray diffraction ($'N_3' =$ tridentate cyclic triamine or podal pyridine-amine-pyridine ligand). Their electrochemical oxidation and their oxygenation by H_2O_2 and O_2 have been investigated. The σ-donor capacity of ligand $'N_3'$ in $[{}'N_3'Rh^{I}(cod)]^{+}$ strongly influences the electrochemical oxidation potential and the ^{13}C chemical shift of the cod double bond. The relative σ-donor strength of the individual amine (N^{R}_{amine}) and pyridine (N_{Py}) nitrogens in the pyridine-amine-pyridine ligands, $N^{H}_{amine} > N_{Py} > N_{Py\text{-}Me} > N^{Bu}_{amine} \cong N^{Bz}_{amine}$, is largely determined by steric repulsions. The cod complexes are selectively oxygenated by H_2O_2, and in one case by O_2, to rhodium(III)oxabicyclononadiyl complexes which rearrange to rhodium(III)-hydroxycyclooctenediyl complexes. Oxygenation of cod to an oxabicyclononadiyl fragment and subsequent rearrangement to a hydroxycyclooctenediyl fragment are both thought to proceed via a 2-rhodaoxetane intermediate. Oxygenation of $[{}'N_3'Rh^{I}(cod)]^{+}$ by H_2O_2 is relatively independent of the ligand and the solvent, and proceeds instantaneously and selectively. Oxygenation of $[{}'N_3'Rh^{I}(cod)]^{+}$ by O_2 is greatly influenced by both the ligand and the solvent. Entirely selective oxidation by O_2 could only be obtained for $'N_3' = N,N$-di(2-pyridylmethyl)amine (BPA) in CH_2Cl_2. Oxygenation by O_2 in CH_2Cl_2 requires one mole of O_2 per mole of $[(BPA)Rh^{I}(cod)]^{+}$, is catalysed by acid and is likely to proceed by mononuclear activation of dioxygen. For both the cyclic triamine ligands and the podal pyridine-amine-pyridine ligands, the cod complexes with the lowest oxidation potentials are the most reactive and the most selective in oxygenation by O_2. Oxidation of the analogous 1,5-hexadiene (hed) complexes $[{}'N_3'Rh^{I}(hed)]^{+}$ by either H_2O_2 or O_2 results in elimination of hed.

Keywords: alkene complexes · oxygen · oxygenations · peroxides · rhodium

Introduction

Transition metal mediated oxidation of olefins by the environmentally friendly oxidants H_2O_2 or O_2 (air) is of great (industrial) importance.[1] For economic reasons, bulk oxidation of alkenes to give useful industrial chemicals predominantly involves the use of O_2 as the primary oxidant.[2] Also in fine-chemical processes clean oxidants are increasingly desirable. However, both H_2O_2 and O_2 have a tendency to oxidise by mechanisms that are poorly understood and therefore are not readily controlled.[3] In oxidation with O_2, it is a challenge to use both oxygen atoms, as this would circumvent the need for a sacrificial reductant.

[a] Prof. Dr. A. W. Gal, Dipl.-Chem. B. de Bruin, M. J. Boerakker, J. A. Brands, J. J. J. M. Donners, M. P. J. Donners, Dr. R. de Gelder, J. M. M. Smits
Department of Inorganic Chemistry, University of Nijmegen
Toernooiveld 1, 6525 ED Nijmegen (The Netherlands)
E-mail: gal@sci.kun.nl

[b] Dr. A. L. Spek
Department of Crystal and Structural Chemistry
Bijvoet Centre for Biomolecular Research, University of Utrecht
Padualaan 8, 3584 CH Utrecht (The Netherlands)

Homogeneous catalytic activity of rhodium in the oxidation of olefins by O_2 and H_2O_2 has been demonstrated. Selective oxidation of linear olefins to ketones by O_2, H_2O_2 or *t*BuOOH[4] and oxidation of tetramethylethylene to the epoxide by *t*BuOOH have been reported.[5] Cyclic olefins and styrene have been oxidised with O_2 to give a variety of products, including ketones and epoxides.[6] Mechanistic proposals for these catalytic conversions are controversial.

In metal-catalysed oxidation of olefins, 2-metallaoxetanes have often been proposed as crucial intermediates. Remarkably, 2-rhodaoxetanes have not been invoked as intermediates in the above-mentioned catalytic oxidations with rhodium. For iridium we are aware of one example of stoichiometric oxidation of a coordinated olefin, in which $[(P_3O_9)Ir^{I}(cod)]^{2-}$ is oxidised by O_2 to a 2-irida(III)oxetane.[7] Rearrangement of this 2-irida(III)oxetane results in an Ir^{III}(2-hydroxycycloocta-4-ene-1,6-diyl) complex. In contrast, oxidation of $[\{(cod)Ir^{I}(\mu\text{-}Cl)\}_2]$ by air does not result in oxygenation of the cod; the dinuclear oxohydroxo complex $[Ir^{III}_2Cl_2(cod)_2(\mu\text{-}OH)_2(\mu\text{-}O)]$ is formed.[8] $[\{(cod)Ir^{III}(H)(Cl)(\mu\text{-}Cl)\}_2]$, the HCl adduct of $[\{(cod)Ir^{I}(\mu\text{-}Cl)\}_2]$, has been reported to eliminate 4-cyclooctene-1-one upon reaction with O_2.[9] A $\{(cod)Ir^{III}(OOH)\}$ moiety was postulated as an intermediate.

In this paper we report the electrochemical oxidation of complexes $[{}'N_3{}'Rh^I(cod)]^+$ (cod = *Z*,*Z*-1,5-cyclooctadiene) and their oxidation by H_2O_2 and O_2 via a 2-rhodaoxetane intermediate. In these complexes the stabilising ligand $'N_3'$ is a tridentate cyclic triamine or podal pyridine-amine-pyridine ligand. Part of this work has been communicated previously.[10]

Results

Synthesis of the diolefin complexes: We synthesised the cationic cod complex [**1**]$^+$ by the route shown in Scheme 1. Stirring 1,4,7-triazacyclononane (Cn) with $[\{(cod)Rh(\mu\text{-}Cl)\}_2]$ in a molar ratio 2:1 in methanol at room temperature resulted in the formation of [**1**]Cl. Addition of NH_4PF_6 to the obtained solution resulted in the precipitation of [**1**]PF_6. Similarly, addition of $NaBPh_4$ to the solution of [**1**]Cl in methanol resulted in the precipitation of [**1**]BPh_4. The $'N_3'$-ligand complexes [**2**]$^+$–[**7**]$^+$ and the $'N_2'$ ligand complex [**9**]$^+$, were also obtained as their PF_6^- or BPh_4^- salts (Scheme 1). The dinuclear complex [**8**]$^{2+}$ was generated by reaction of $[\{(cod)Rh(\mu\text{-}Cl)\}_2]$ with the ditopic ligand TPBN in a 1:1 molar ratio and was isolated as [**8**][PF_6]$_2$.

The 1,5-hexadiene (hed) complexes [**10**]$^+$ and [**11**]$^+$ were generated by reaction of $[\{(hed)Rh(\mu\text{-}Cl)\}_2]$ with Cn* and BzBLA, respectively. They were precipitated as PF_6^- salts (Scheme 2). The complexes in Schemes 1 and 2 are all five coordinate, with the exception of square-planar complex [**9**]$^+$.

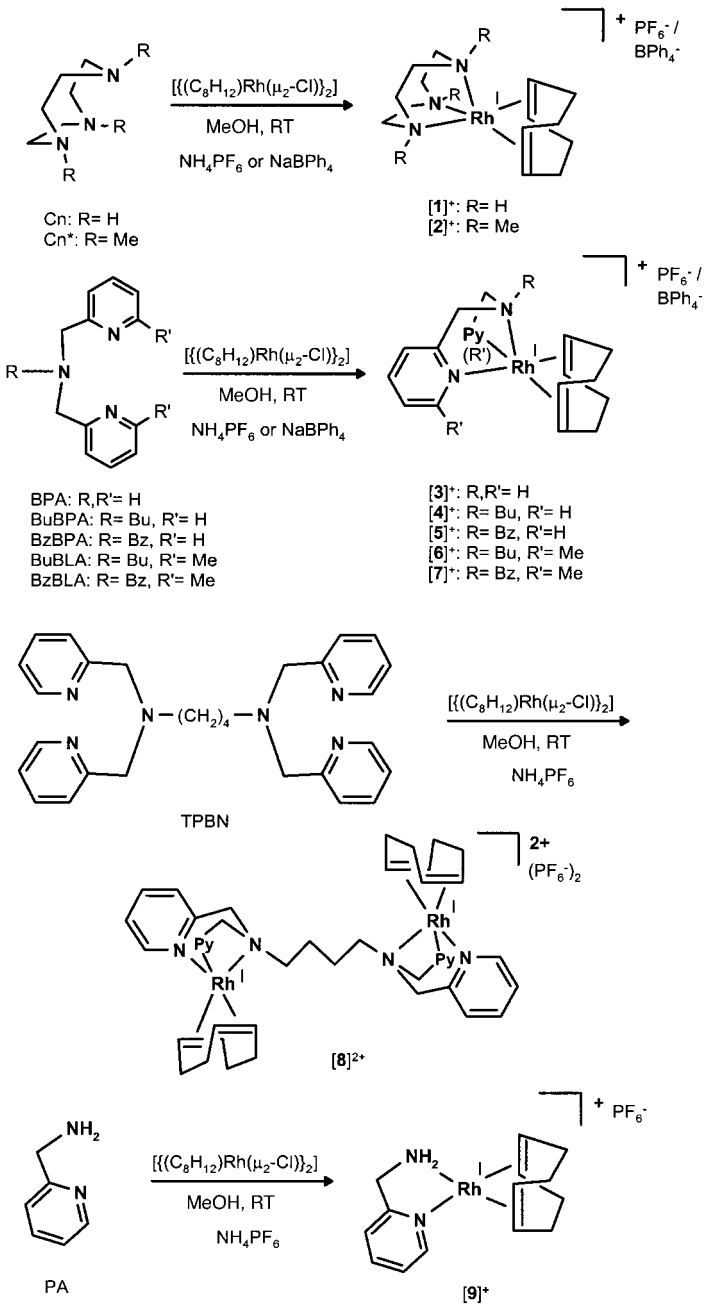

Scheme 1. Preparation of Rh^I(cod) cations [**1**]$^+$–[**9**]$^+$.

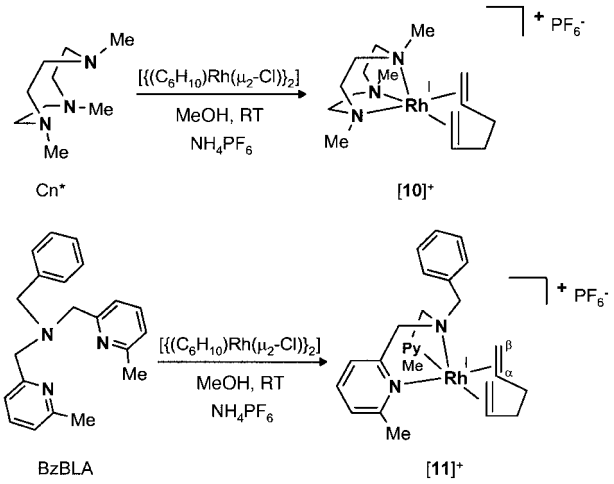

Scheme 2. Preparation of Rh^I(hed) cations [**10**]$^+$ and [**11**]$^+$.

NMR data of the diolefin complexes: The cod complexes [**1**]$^+$–[**9**]$^+$ (Scheme 1) are all highly fluxional in solution. The η^4-cod fragments appear to rotate fast on the NMR timescale. The two −HC=CH− fragments of cod are observed as one signal, both in ^{1}H and ^{13}C NMR spectra. The fluxionality observed for the five-coordinate complexes [**1**]$^+$–[**8**]$^+$ is thought to be a rapid equilibrium between trigonal-bipyramidal and square-pyramidal coordination geometries through rotation of cod (Scheme 3, path a). For complex

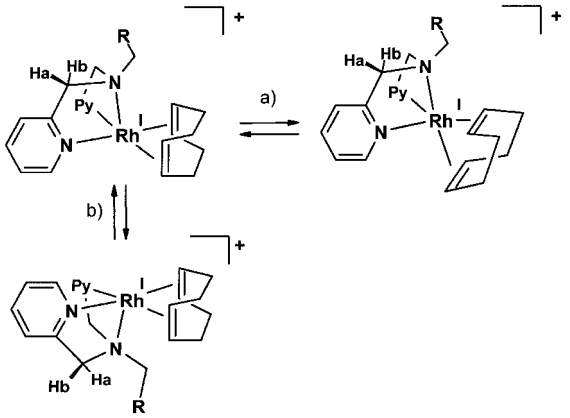

Scheme 3. Fluxional behaviour of five-coordinate complex [**4**]$^+$. a) Fast equilibrium between square pyramidal and trigonal bipyramidal coordination geometry through rotation of cod. b) Slow equilibrium involving dissociation, pyramidal inversion and recoordination of N^R_{amine}.

0947-6539/99/0510-2922 $ 17.50+.50/0 *Chem. Eur. J.* **1999**, *5*, No. 10

[**4**]$^+$, we attempted to freeze this process by cooling. However, at 500 MHz this process is still fast at $-90\,^\circ$C. Below $-90\,^\circ$C the [D$_6$]acetone became too viscous to obtain a solution NMR spectrum.

In the ^{1}H NOESY/EXSY spectrum of [**11**]$^+$, NOE contacts are observed between the Py−*CH*$_3$ group and the α-vinylic η^4-hed proton −*CH*=CH$_c$H$_t$, but there is no interaction with the β-vinylic *cis*- (H$_c$) or *trans*- (H$_t$) hed protons −CH=*CH$_c$H$_t$*. The benzylic methylene fragment, N−CH$_2$−Ph, has a clear NOE contact with the β-vinylic H$_c$ and H$_t$ protons and no interaction with the α-vinylic protons. No exchange correlations were observed in the ^{1}H NOESY/EXSY spectrum. Thus, the predominant structure of [**11**]$^+$ in solution appears to be the five-coordinate structure drawn in Scheme 2.

The complexes [**3**]$^+$–[**8**]$^{2+}$ and [**11**]$^+$, with pyridine-amine-pyridine ligands, have very characteristic ^{1}H NMR spectra. For complexes [**3**]$^+$–[**5**]$^+$ and [**8**]$^{2+}$, the chemical shifts of the Py−H6 signals ($\delta = 9.2-9.3$), which are downfield relative to those of the free ligands ($\delta = 8.5-8.6$), indicate that both pyridyl donors are coordinated in solution. Similarly, for complexes [**6**]$^+$, [**7**]$^+$ and [**11**]$^+$ the downfield chemical shifts of the Py−Me signals ($\delta = 3.5-3.6$), relative to the free ligands ($\delta = 2.5$), reveal coordination of both methyl-substituted pyridyl donors (N$_{Py\text{-}Me}$). In marked contrast, the Py−H6 signal in the square planar compound [**9**]$^+$ ($\delta = 7.8$), has shifted upfield relative to the free pyridine-amine ligand ($\delta = 8.5$); this is probably due to anisotropic shielding by the olefin fragment that is coordinated perpendicularly to the pyridine plane. In the ^{1}H NMR spectra of [**3**]$^+$–[**8**]$^{2+}$ and [**11**]$^+$, the diastereotopic methylene protons of the N-CH$_2$-Py or N-CH$_2$-PyMe fragments give rise to two AB type doublets. This confirms coordination of the central amine donor (N$_{amine}$). In the ^{1}H NOESY/EXSY spectrum of [**8**]$^{2+}$, NOE contacts are observed between the vinylic protons of the cod fragments and both Py−H6 and α-CH$_2$ of the N-(CH$_2$)$_4$-N tether. The above NMR data clearly indicate κ^3-coordination of the pyridine-amine-pyridine ligands.

The two AB type doublets of the diastereotopic methylene protons of the N-CH$_2$-Py fragments in [**8**]$^{2+}$ show an exchange correlation in the ^{1}H NOESY/EXSY spectrum. At 90 MHz, the two AB type doublets of both complexes [**8**]$^{2+}$ and [**4**]$^+$ (^{1}H NMR) start to coalesce into a broad singlet at approximately 77 °C. These observations indicate dissociation, pyramidal inversion and recoordination of N$^R_{amine}$ (Scheme 3, path b).

X-ray structures of the cod complexes: The X-ray structures of the complexes [**2**]$^+$, [**3**]$^+$, [**6**]$^+$, [**7**]$^+$ and [**8**]$^{2+}$ (Scheme 1) confirm that they are all five-coordinate in the solid state (see Figures 1–5). For both [**6**]$^+$ and [**7**]$^+$ two independent cations, [**6^A**]$^+$/[**6^B**]$^+$ and [**7^A**]$^+$/[**7^B**]$^+$ are found per unit cell. Selected bond lengths and angles are summarised in Tables 1 and 2.

The structures all deviate from ideal trigonal-bipyramidal or square-pyramidal geometries. Nevertheless, we classified their geometry as either pseudo trigonal bipyramidal or pseudo square pyramidal, based on the root-mean-square deviation of the observed coordination angles from those in ideal geometries. Coordination angles, constrained by the backbones of the cod and N ligands, were not taken into account.

Complex [**2**]$^+$ (Figure 1) adopts a trigonal-bipyramidal coordination geometry in the solid state. Two N$^{Me}_{amine}$ donors of Cn* (N1 and N2) and a double bond of cod (C11−C12) occupy the equatorial positions; the third N$^{Me}_{amine}$ of Cn* (N3)

Table 1. Selected bond lengths [Å] for [**2**]$^+$, [**3**]$^+$, [**6^A**]$^+$/[**6^B**]$^+$, [**7^A**]$^+$/[**7^B**]$^+$, [**8**]$^{2+}$, [**15^A**]$^+$/[**15^B**]$^+$ and [**16a**]$^+$.[a]

	[**2**]$^+$	[**3**]$^+$	[**6^A**]$^+$	[**6^B**]$^+$	[**7^A**]$^+$	[**7^B**]$^+$	[**8**]$^{2+}$	[**12**]$^+$	[**15^A**]$^+$	[**15^B**]$^+$	[**16a**]$^+$
N1−Rh1	2.339(2)	2.218(2)	2.141(4)	2.151(4)	2.135(9)	2.138(8)	2.138(2)	2.228(3)	2.217(6)	2.217(6)	2.123(5)
N2−Rh1	2.335(2)	2.320(2)	2.273(4)	2.302(4)	2.282(8)	2.276(8)	2.155(2)	2.219(4)	2.314(6)	2.314(6)	2.165(4)
N3−Rh1	2.198(2)	2.119(2)	2.397(4)	2.390(4)	2.422(8)	2.408(7)	2.430(2)	2.098(3)	2.237(6)	2.237(6)	2.141(4)
C11−Rh1	2.083(3)	2.084(3)	2.086(5)	2.083(5)	2.096(10)	2.104(11)	2.088(3)	2.069(4)	2.090(15)	2.109(12)	2.069(6)
C12−Rh1	2.076(3)	2.063(3)	2.100(5)	2.100(5)	2.101(11)	2.105(10)	2.118(3)	2.617(5)			
C21−Rh1	2.158(3)	2.139(3)	2.150(4)	2.152(5)	2.153(10)	2.128(10)	2.122(3)	2.052(4)	2.135(17)	2.186(13)	2.167(6)
C22−Rh1	2.169(3)	2.148(3)	2.177(4)	2.153(5)	2.183(10)	2.161(10)	2.134(3)	2.605(4)	2.074(14)	2.090(14)	2.186(7)
C23−Rh1									2.117(13)	2.227(19)	2.148(7)
Rh1−O1								2.077(3)			
C12−O1								1.515(5)	1.416(19)	1.401(18)	1.535(11)
C22−O1								1.503(5)			
C11−C12	1.436(5)	1.401(6)	1.426(8)	1.412(8)	1.436(15)	1.427(15)	1.416(4)	1.522(6)	1.533(17)	1.522(17)	1.529(9)
C21−C22	1.381(4)	1.404(6)	1.387(7)	1.373(8)	1.401(15)	1.385(16)	1.404(4)	1.519(6)	1.467(18)	1.457(17)	1.517(11)
C11−C14	1.520(4)	1.511(6)	1.505(7)	1.525(7)	1.518(14)	1.495(15)	1.515(4)	1.520(6)	1.524(19)	1.530(18)	1.441(10)
C21−C24	1.499(5)	1.499(8)	1.522(7)	1.502(7)	1.496(15)	1.502(15)	1.513(4)	1.524(6)	1.53(2)	1.520(19)	1.472(10)
C12−C13	1.511(4)	1.503(5)	1.530(7)	1.497(9)	1.498(16)	1.527(17)	1.523(4)	1.520(7)	1.458(19)	1.441(18)	1.418(11)
C22−C23	1.508(5)	1.491(6)	1.502(7)	1.517(8)	1.522(16)	1.524(16)	1.502(4)	1.528(7)	1.371(17)	1.373(18)	1.387(9)
C14−C24	1.524(5)	1.487(9)	1.517(7)	1.474(8)	1.539(15)	1.532(15)	1.537(5)	1.538(7)	1.54(2)	1.526(19)	1.531(11)
C13−C23	1.527(5)	1.494(6)	1.500(8)	1.447(10)	1.550(17)	1.47(2)	1.516(5)	1.553(7)	1.470(19)	1.47(2)	1.533(9)
N3−C51	1.509(4)	1.475(4)	1.467(6)	1.480(6)	1.477(13)	1.467(12)	1.469(4)	1.495(5)	1.483(10)	1.483(10)	1.476(7)
N1−C52	1.485(4)	1.346(3)	1.364(6)	1.355(7)	1.343(13)	1.345(13)	1.339(4)	1.492(6)	1.464(11)	1.464(11)	1.341(8)
N3−C61	1.493(4)	1.482(3)	1.474(6)	1.469(5)	1.467(11)	1.473(11)	1.469(4)	1.507(6)	1.452(13)	1.452(13)	1.490(7)
N2−C62	1.493(4)	1.338(3)	1.354(6)	1.363(6)	1.380(13)	1.348(13)	1.339(4)	1.478(6)	1.44(2)	1.44(2)	1.345(7)
C51−C52	1.504(5)	1.494(4)	1.504(7)	1.511(7)	1.509(13)	1.513(13)	1.504(4)	1.497(6)	1.345(14)	1.345(14)	1.500(8)
C61−C62	1.505(5)	1.499(4)	1.517(6)	1.503(6)	1.506(14)	1.497(13)	1.505(4)	1.509(6)	1.39(2)	1.39(2)	1.500(7)

[a] For atom labelling see Figures 1–5, 7, 8 and 9.

Table 2. Selected bond angles [°] for $[\mathbf{2}]^+$, $[\mathbf{3}]^+$, $[\mathbf{6^A}]^+/[\mathbf{6^B}]^+$, $[\mathbf{7^A}]^+/[\mathbf{7^B}]^+$, $[\mathbf{8}]^{2+}$, $[\mathbf{15^A}]^+/[\mathbf{15^B}]^+$ and $[\mathbf{16a}]^+$.[a]

	$[\mathbf{2}]^+$	$[\mathbf{3}]^+$	$[\mathbf{6^A}]^+$	$[\mathbf{6^B}]^+$	$[\mathbf{7^A}]^+$	$[\mathbf{7^B}]^+$	$[\mathbf{8}]^{2+}$	$[\mathbf{12}]^+$	$[\mathbf{15^A}]^+$	$[\mathbf{15^B}]^+$	$[\mathbf{16a}]^+$
N1-Rh1-N2	76.77(9)	75.77(8)	90.44(14)	91.57(13)	90.2(3)	87.3(3)	85.37(9)	80.37(13)	79.4(3)	79.4(3)	81.32(16)
N1-Rh1-N3	80.09(9)	78.13(8)	73.78(14)	74.66(15)	73.5(3)	73.5(3)	76.09(9)	81.87(13)	79.5(2)	79.5(2)	77.85(18)
N2-Rh1-N3	78.91(9)	77.35(8)	74.84(14)	74.14(13)	74.6(3)	75.2(3)	74.76(9)	82.14(13)	79.3(3)	79.3(3)	80.45(16)
N1-Rh1-C11	125.55(11)	130.96(14)	89.49(17)	89.52(17)	91.1(4)	92.4(4)	93.33(11)	102.13(15)	91.5(4)	103.4(4)	93.1(2)
N1-Rh1-C12	163.51(11)	167.16(12)	89.34(17)	89.62(19)	88.4(4)	88.0(4)	92.21(11)	97.86(14)			
N1-Rh1-C21	87.78(10)	89.43(11)	157.97(17)	160.91(18)	160.9(4)	161.7(4)	170.07(9)	171.45(15)	104.5(4)	171.2(4)	108.8(3)
N1-Rh1-C22	111.81(11)	110.53(12)	163.58(17)	160.83(19)	160.6(3)	160.0(4)	151.36(10)	135.86(14)	142.6(4)	131.5(4)	144.9(2)
N1-Rh1-C23									172.7(4)	104.7(5)	175.4(2)
N2-Rh1-C11	155.66(11)	148.24(15)	174.86(18)	178.63(18)	178.6(4)	178.7(4)	175.68(11)	173.39(14)	170.4(4)	172.7(4)	173.9(2)
N2-Rh1-C12	115.78(11)	110.82(13)	135.05(18)	139.71(18)	139.6(4)	139.1(4)	144.75(11)	138.42(14)			
N2-Rh1-C21	113.54(11)	122.00(17)	100.70(16)	98.17(16)	97.5(4)	100.2(4)	98.35(11)	99.42(16)	102.0(5)	97.8(4)	103.1(2)
N2-Rh1-C22	91.02(11)	95.60(11)	88.43(17)	87.06(17)	89.1(4)	91.2(4)	85.64(10)	99.80(14)	93.4(4)	88.2(4)	89.1(2)
N2-Rh1-C23									107.9(4)	109.4(5)	103.2(2)
N3-Rh1-C11	94.44(11)	90.76(12)	110.04(17)	106.96(17)	106.2(4)	105.9(4)	100.93(11)	104.21(15)	96.1(4)	94.4(4)	95.9(2)
N3-Rh1-C12	91.54(11)	92.34(11)	146.68(18)	143.98(18)	142.4(4)	141.0(3)	138.61(10)	139.13(14)			
N3-Rh1-C21	160.26(11)	153.92(17)	90.71(16)	92.19(17)	91.6(4)	92.1(4)	95.93(10)	106.61(15)	176.0(4)	108.3(4)	172.7(2)
N3-Rh1-C22	162.44(11)	167.43(14)	121.53(16)	123.00(17)	124.7(4)	125.3(4)	127.12(10)	142.21(14)	135.6(4)	144.0(4)	133.9(2)
N3-Rh1-C23									102.5(4)	170.8(5)	101.8(2)
C11-Rh1-C12	40.41(13)	39.48(17)	39.8(2)	39.4(2)	40.0(4)	39.6(4)	39.33(12)	35.52(15)			
C21-Rh1-C22	37.22(12)	38.23(17)	37.39(19)	37.2(2)	37.7(4)	37.7(4)	38.54(11)	35.62(15)	40.8(5)	39.8(5)	40.8(3)
C21-Rh1-C23									73.5(5)	68.2(5)	71.3(3)
C21-Rh1-C11	79.96(12)	80.14(17)	81.09(19)	81.03(19)	81.4(4)	80.5(4)	82.27(11)	77.18(17)	83.2(6)	80.5(5)	81.0(3)
C21-Rh1-C12	96.06(12)	95.77(14)	95.84(18)	93.4(2)	96.7(4)	96.8(4)	89.99(12)	76.55(16)			
C22-Rh1-C23									38.2(5)	36.9(5)	37.3(3)
C22-Rh1-C11	88.87(13)	90.01(13)	90.2(2)	91.6(2)	89.5(4)	88.7(4)	97.38(12)	74.10(16)	95.7(5)	94.7(5)	96.9(3)
C22-Rh1-C12	79.84(12)	80.34(14)	80.0(2)	79.3(4)	79.6(4)	80.2(4)	79.83(11)	53.39(15)			
C23-Rh1-C11									81.3(5)	76.6(5)	82.4(2)
Rh1-C11-C12	69.54(17)	69.44(18)	70.6(3)	70.9(3)	70.2(6)	70.2(6)	71.45(17)	92.3(3)	111.3(10)	114.1(9)	108.0(5)
Rh1-C21-C22	71.84(18)	71.23(19)	72.3(3)	71.5(3)	72.3(6)	72.5(6)	71.18(16)	92.5(3)	67.4(8)	66.5(7)	68.9(4)
Rh1-C12-C11	70.05(17)	71.1(2)	69.6(3)	69.6(3)	69.8(6)	70.1(6)	69.22(17)	52.2(2)	71.9(9)	73.7(8)	
Rh1-C22-C21	70.95(17)	70.5(2)	70.3(3)	71.3(3)	70.0(6)	69.9(6)	70.29(16)	51.9(2)	72.6(8)	73.7(8)	69.9(4)
Rh1-C22-C23									72.6(8)	77.0(10)	69.8(4)
Rh1-C23-C22									69.2(8)	66.1(9)	72.8(4)
C21-C22-O1								103.8(3)			
C11-C12-O1								103.8(3)	111.6(13)	113.3(12)	110.1(6)
C22-O1-Rh1								92.0(2)			
C12-O1-Rh1								92.2(2)			
C14-C11-C12	122.4(3)	122.1(4)	121.9(5)	122.9(5)	121.6(9)	123.7(10)	123.3(3)	116.8(4)	108.6(13)	108.4(12)	116.6(7)
C11-C12-C13	124.1(3)	124.3(4)	125.2(5)	124.1(6)	125.6(10)	123.4(10)	121.9(3)	119.6(4)	114.9(13)	112.4(12)	114.0(6)
C12-C13-C23	111.7(3)	113.1(3)	113.5(5)	115.0(5)	112.1(9)	113.0(10)	111.2(3)	104.7(4)	115.6(13)	114.4(13)	114.5(6)
C24-C14-C11	110.9(3)	111.3(4)	112.6(4)	115.0(4)	111.6(8)	112.4(9)	112.5(2)	110.6(4)	110.0(13)	109.5(11)	113.9(6)
C22-C21-C24	124.9(3)	125.6(4)	125.2(5)	124.7(5)	125.2(10)	123.6(10)	123.1(3)	115.8(4)	122.8(15)	122.2(12)	122.0(7)
C23-C22-C21	123.7(3)	122.0(3)	122.3(5)	123.2(5)	122.5(10)	125.1(10)	125.6(3)	120.2(4)	127.4(12)	121.9(13)	119.9(6)
C13-C23-C22	112.4(3)	112.6(3)	112.3(4)	114.4(5)	110.4(9)	113.7(9)	111.8(2)	105.3(4)	132.0(14)	131.8(16)	125.9(6)
C21-C24-C14	112.7(3)	113.8(3)	113.1(4)	114.7(4)	112.6(9)	112.2(9)	113.0(3)	108.9(4)	114.8(14)	111.5(13)	107.7(6)
Rh1-N1-C52	98.79(18)	112.33(17)	113.1(3)	113.9(3)	113.7(6)	115.2(6)	119.52(18)	107.7(3)	107.3(5)	107.3(5)	116.0(4)
N1-C52-C51	112.6(3)	115.8(2)	117.2(4)	117.9(4)	118.7(8)	116.0(8)	120.4(3)	111.0(4)	121.4(8)	121.4(8)	115.0(5)
C52-C51-N3	112.1(3)	111.2(2)	110.4(4)	110.5(4)	109.3(8)	109.6(8)	115.6(3)	112.1(4)	119.5(7)	119.5(7)	110.1(4)
C51-N3-Rh1	109.94(19)	108.77(16)	98.1(3)	99.4(3)	98.2(6)	97.5(5)	108.01(18)	104.2(3)	105.9(5)	105.9(5)	109.2(3)
Rh1-N2-C62	107.55(19)	111.12(17)	115.7(3)	114.3(3)	114.8(6)	115.8(6)	119.04(19)	101.7(3)	104.1(8)	104.1(8)	112.3(3)
N2-C62-C61	112.0(3)	116.4(2)	118.0(4)	115.2(4)	116.6(8)	119.5(8)	116.6(3)	110.9(4)	122.6(11)	122.6(11)	115.9(4)
C62-C61-N3	112.0(3)	112.5(2)	112.7(4)	111.1(4)	112.4(9)	115.6(8)	113.0(2)	111.9(4)	120.3(11)	120.3(11)	111.9(4)
C61-N3-Rh1	103.89(18)	111.08(16)	106.9(3)	107.4(3)	105.3(5)	107.4(5)	103.43(17)	110.4(3)	108.2(7)	108.2(7)	108.2(3)

[a] For atom labelling see Figures 1–5, 7, 8 and 9.

and the other double bond of cod (C21–C22) occupy the axial positions.

Complex $[\mathbf{3}]^+$ (Figure 2) adopts an asymmetric square-pyramidal geometry. The two cod double bonds (C11–C12 and C21–C22), one of the pyridine nitrogens, N_{Py} (N1), and N^{H}_{amine} (N3) are coordinated in the basal plane. The second N_{Py} (N2) is coordinated at the apical position.

The complexes $[\mathbf{6^A}]^+/[\mathbf{6^B}]^+$ (Figure 3) and $[\mathbf{7^A}]^+/[\mathbf{7^B}]^+$ (Figure 4) adopt an asymmetric trigonal-bipyramidal geometry. In these complexes N_{amine} (N3), together with one of the 2-methylpyridyl donors, $N_{Py\text{-}Me}$ (N2), and a cod double bond (C11–C12) span the equatorial plane. The second $N_{Py\text{-}Me}$ (N1) and the other cod double bond (C21–C22) are coordinated axially.

The dinuclear complex $[\mathbf{8}]^{2+}$ (Figure 5) adopts a symmetric square pyramidal geometry. The two cod double bonds (C11–C12 and C21–C22) and the two N_{Py} (N1 and N2) are coordinated in the basal plane. The amine nitrogen, $N^{\text{“Bu”}}_{amine}$ (N3) is coordinated at the apical position.

0947-6539/99/0510-2924 $ 17.50+.50/0 *Chem. Eur. J.* **1999**, *5*, No. 10

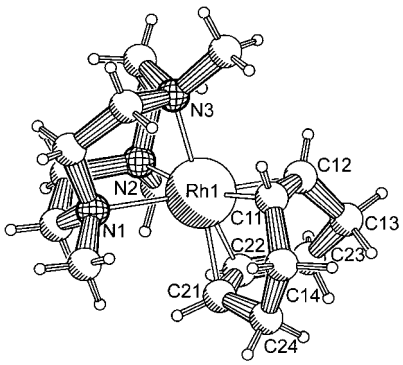

Figure 1. X-ray structure of trigonal bipyramidal complex $[\mathbf{2}]^+$.

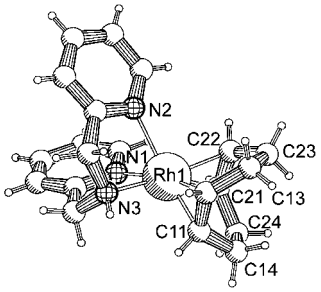

Figure 2. X-ray structure of asymmetric square pyramidal complex $[\mathbf{3}]^+$.

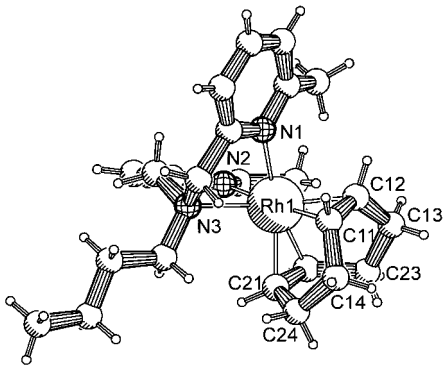

Figure 3. X-ray structure of asymmetric trigonal bipyramidal complex $[\mathbf{6^A}]^+$.

For d^8 metals in a trigonal-bipyramidal geometry, theoretical and experimental results by Rossi and Hoffmann indicate that the strongest σ donor prefers the axial position and that olefins bind more strongly in the equatorial position.[11] Apparently, $N_{Py\text{-}Me}$ is a stronger σ-donor than N^{R}_{amine} (R = Bu, Bz) in $[\mathbf{6^A}]^+/[\mathbf{6^B}]^+$ and $[\mathbf{7^A}]^+/[\mathbf{7^B}]^+$. In accordance with the predictions of Rossi and Hoffmann, the equatorial metal–olefin interactions in $[\mathbf{2}]^+$ and $[\mathbf{6^A}]^+/[\mathbf{6^B}]^+$ are the strongest, as indicated by the significantly shorter Rh–C distances of the equatorial cod double bond (Rh1–C11 and Rh1–C12) relative to the axial cod double bond

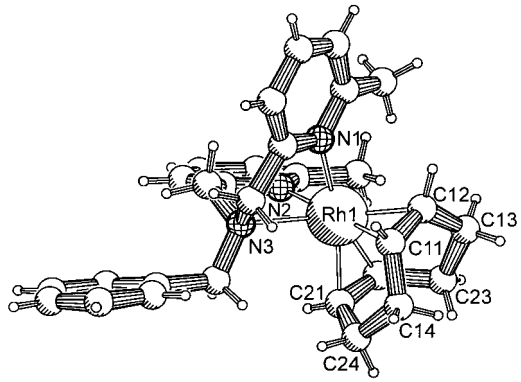

Figure 4. X-ray structure of asymmetric trigonal bipyramidal complex $[\mathbf{7^A}]^+$.

(Rh1–C21 and Rh1–C22). For $[\mathbf{7^A}]^+$ and $[\mathbf{7^B}]^+$ the Rh–C distances for these two positions are not significantly different (see Table 1). As expected, the axial C–C distance (C21–C22) in $[\mathbf{2}]^+$ is shorter than the equatorial (C11–C12). Axial and equatorial C–C distances are not significantly different for $[\mathbf{6^A}]^+/[\mathbf{6^B}]^+$ and $[\mathbf{7^A}]^+/[\mathbf{7^B}]^+$.

For d^8 metals in a square-pyramidal geometry, Rossi and Hoffmann have shown that the strongest σ-donor ligand prefers the basal position and that olefins also interact more strongly in the basal position.[11] The X-ray structure of $[\mathbf{3}]^+$ therefore seems to indicate that N^{H}_{amine} (N3) is a stronger σ donor than N_{Py}. Apparently, the tertiary amine $N^{\text{“Bu”}}_{amine}$ (N3) is the weaker σ donor in $[\mathbf{8}]^{2+}$. Based on the X-ray data the relative donor strength of the nitrogen atoms in the above pyridine-amine-pyridine ligands appears to be: $N^{H}_{amine} > N_{Py} > N^{Bu}_{amine}$ and $N_{Py\text{-}Me} > N^{Bu}_{amine} \cong N^{Bz}_{amine}$.

The equatorial Rh–N distances for N_{amine} (2.335–2.422 Å) and $N_{Py\text{-}Me}$ (2.273–2.302 Å) of $[\mathbf{2}]^+$, $[\mathbf{6^A}]^+/[\mathbf{6^B}]^+$ and $[\mathbf{7^A}]^+/[\mathbf{7^B}]^+$ are long relative to the reported Rh–N_{sp2} (2.007–2.140 Å)[12] and Rh–N_{sp3} (2.111–2.178 Å)[12f, 13] distances for square planar [′N_2′Rh^I(cod)] complexes. The few X-ray structures of five-coordinate [′N_3′Rh^I(cod)] and [′N_3′Rh^I(nbd)] (nbd = norbornadiene) complexes reported thus far are all trigonal bipyramidal and contain only N_{sp2} donors. Their Rh–N_{sp2} distances (axial: 2.096–2.166 Å; equatorial 2.16–2.293 Å) compare quite well with the Rh–$N_{Py\text{-}Me}$ distances in $[\mathbf{6^A}]^+/[\mathbf{6^B}]^+$ and $[\mathbf{7^A}]^+/[\mathbf{7^B}]^+$ (axial: 2.135–2.151 Å; equatorial: 2.273–2.302 Å).[14]

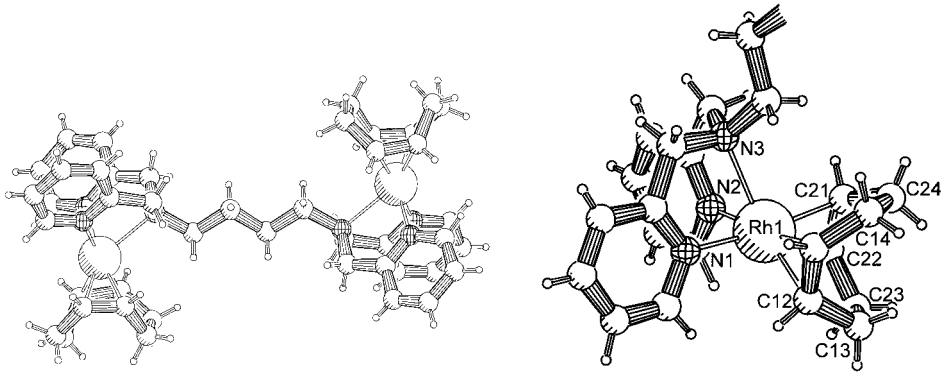

Figure 5. X-ray structure of symmetric square pyramidal dinuclear complex $[\mathbf{8}]^{2+}$. Left: relative position of the two rhodium centres. Right: detailed coordination geometry of each rhodium centre.

Electrochemical oxidation of the diolefin complexes: Electrochemical oxidation of the cod complexes $[\mathbf{1}]^+ - [\mathbf{9}]^+$ (Scheme 1) was studied by means of cyclic voltammetry. For complexes $[\mathbf{1}]^+$, $[\mathbf{3}]^+$, $[\mathbf{6}]^+$ and $[\mathbf{7}]^+$ in CH_2Cl_2 (0.1M TBAH) a reversible, one-electron oxidation was observed at 100 mV s^{-1}. The other complexes were oxidised irreversibly at this scan rate. Table 3 gives for each complex the ^{13}C chemical shift of the olefinic cod fragments ($\delta(^{13}C_{C=C})$) and the anodic peak potential (E^p_{anode}) of the observed oxidation wave. For the reversible oxidations the halfwave potentials ($E_{1/2}$) and the peak separations (ΔE) are also listed. The 1,5-hexadiene complex $[\mathbf{10}]^+$ (Scheme 2) is oxidised more easily (irreversibly; $E^p_{anode} = 141$ mV) than its cod analogue $[\mathbf{2}]^+$ (irreversibly; $E^p_{anode} = 225$ mV).

Table 3. E^p_{anode} and $\delta(^{13}C_{(C=C)})$ for $[(L)Rh^I(cod)]+$ complexes.

	L	$\delta(^{13}C_{(C=C)})$	E^p_{anode}[a]	$E_{1/2}$[a,b]	ΔE[a,b]
$[\mathbf{1}]^+$	Cn	69.2	−5	−38	66
$[\mathbf{3}]^+$	BPA	72.3	119	86	66
$[\mathbf{3}]^+ + 1$ equiv H^+ ($[\mathbf{18}]^{2+}$)	BPAH^+	84.1[c]	136	–	–
$[\mathbf{2}]^+$	Cn*	74.2	225	–	–
$[\mathbf{4}]^+$	BuBPA	75.9	265	–	–
$[\mathbf{5}]^+$	BzBPA	76.2	296	–	–
$[\mathbf{6}]^+$	BuBLA	76.5	300	270	60
$[\mathbf{7}]^+$	BzBLA	77.2	341	307	68
$[\{Rh(cod)(\mu\text{-}Cl)\}_2]$	Cl^-	78.5[d]	457	–	–
$[\mathbf{9}]^+$	PA	82.6	597	–	–

[a] Measured in CH_2Cl_2 (0.1M TBAH); Potentials in mV vs. the Fc/Fc^+ couple. [b] In case of electrochemically reversible oxidations. [c] Average of the four observed signals at −48 °C. [d] Taken from ref. [15].

Owing to its cationic nature, four-coordinate $[\mathbf{9}]^+$ (Scheme 1) is oxidised at a higher potential than four-coordinate $[\{Rh^I(cod)(\mu\text{-}Cl)\}_2]$. The cationic five coordinate complexes $[\mathbf{1}]^+ - [\mathbf{7}]^+$ are oxidised at lower potentials than that of $[\{Rh^I(cod)(\mu\text{-}Cl)\}_2]$. Addition of one equivalent $[H(OEt_2)_2]B(Ar(CF_3)_2)_4$ ("$HBAr^f_4$")[23] to $[\mathbf{3}]PF_6$ converts $[\mathbf{3}]^+$ to square planar complex $[\mathbf{18}]^{2+}$ (Scheme 5 see below). Quite remarkably, this has virtually no effect on E^p_{anode}. This seems to indicate that the protonated κ^2-BPA deprotonates upon one-electron oxidation and stabilises the resulting Rh^{II} centre by κ^3 coordination.

Figure 6 shows a linear correlation between $\delta(^{13}C_{C=C})$ and E^p_{anode}. The strong influence of the nitrogen-donor ligands on E^p_{anode} seems to indicate that the observed oxidations are metal-centred.[16] The linear relationship between $\delta(^{13}C_{C=C})$ and E^p_{anode} suggests that both reflect the σ-donor capacity of the nitrogen-donor ligand; a higher donor capacity results in a lower E^p_{anode} and a lower $\delta(^{13}C_{C=C})$. Lowering of $\delta(^{13}C_{C=C})$ on going from four-coordinate to five-coordinate [(trispyrazolylborate)Rh^I(cod)] complexes has previously been ascribed to increased π back-bonding to the cod double bond;[17] it seems reasonable to assume that stronger N→Rh donation will result in stronger Rh→C=C back-donation. $\delta(^{13}C_{C=C})$ and E^p_{anode} indicate the following order of donor capacity of the N ligands: Cn > BPA > Cn* > BuBPA > BzBPA ≅ BuBLA > BzBLA ≫ PA. From the combination of these relative ligand-donor capacities with the relative σ-donor strengths of the individual nitrogen-donor atoms derived from the X-ray data, we obtain the following refined order of *σ*-donor strengths: $N^H_{amine} > N_{Py} > N_{Py\text{-}Me} > N^{Bu}_{amine} \cong N^{Bz}_{amine}$.

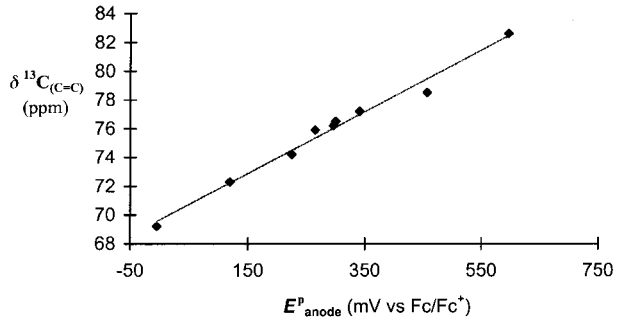

Figure 6. Linear correlation between $\delta(^{13}C_{C=C})$ and E^p_{anode} in a series of $[(L)Rh^I(cod)]^+$ complexes.

The relative σ-donor strengths of the amine and pyridine nitrogens in the above ligands seems to be largely determined by steric repulsion. The order of donor strength $N^H_{amine} > N^{Bu}_{amine} \cong N^{Bz}_{amine}$ and $N_{Py} > N_{Py\text{-}Me}$ finds its parallel in the greater Lewis basicities of secondary amines (R_2NH) relative to tertiary amines (R_3N),[18] and of N_{Py} relative to $N_{Py\text{-}Me}$.[18c]

Oxidation of the diolefin complexes by H_2O_2: Upon reaction of $[\mathbf{2}]PF_6$ with an excess of 35% aqueous H_2O_2 in methanol, the colour of the solution immediately changed from bright yellow to pale yellow. The ^1H NMR spectrum of the pale yellow powder that was obtained by evaporation of the solvent indicated quantitative conversion of $[\mathbf{2}]PF_6$ to $[\mathbf{12}]PF_6$ (Scheme 4).

The X-ray structure of $[\mathbf{12}]^+$ shows that oxygenation of both double bonds of the cod fragment in $[\mathbf{2}]^+$ has resulted in a 9-oxabicyclo[4.2.1]nona-2,5-diyl (oxabicyclononadiyl) fragment (Figure 7). Oxidation of $[\mathbf{2}]^+$ by H_2O_2 in $[D_6]$acetone or CD_3CN gave the same result.

The oxabicyclononadiyl fragment is a tetrahydrofuran derivative. It is connected to rhodium(III) through two Rh–C bonds and a dative O_{ether}→Rh bond. The structure of oxidation product $[\mathbf{12}]^+$ is unprecedented, but has some structural similarity to the 1,4-cycloaddition product of $[\{(cod)Rh(\mu\text{-}Cl)\}_2]$ with hexafluorobut-2-yne.[19] Selected bond lengths and angles are summarised in Tables 1 and 2. The coordination geometry of the rhodium atom is pseudooctahedral. The Rh–C distances (2.052(4) Å and 2.069(4) Å) are normal for Rh^{III} as are the Rh–N distances. The Rh–N3 distance (2.098(3) Å) is shorter than the Rh–N11 and Rh–N21 distance (2.228(3) Å and 2.219(4) Å). This reflects the smaller *trans* influence of O_{ether} relative to the hydrocarbyl carbons. The Rh^{III}–O_{ether} distance (2.077(3) Å) is short relative to previously observed Rh^{III}–O_{ether} distances (2.11–2.28 Å), whereas the O_{ether}–C distances (1.515(5) Å and 1.503(5) Å) are long relative to those for other Rh^{III}-coordinated ethers (1.35–1.49 Å).[20] The observed oxidation bears some resemblance to the stoichiometric permanganate oxidation of 1,5-hexadienes to tetrahydrofurans.[21]

Similar oxidation of $[\mathbf{3}]Cl$ by H_2O_2 in methanol at room temperature results in the instantaneous selective formation of the oxabicyclononadiyl complex $[\mathbf{13a}]Cl$ (Scheme 4). Treatment of the resulting solution with $NaBPh_4$ results in

  0947-6539/99/0510-2926 $ 17.50+.50/0 *Chem. Eur. J.* **1999**, *5*, No. 10

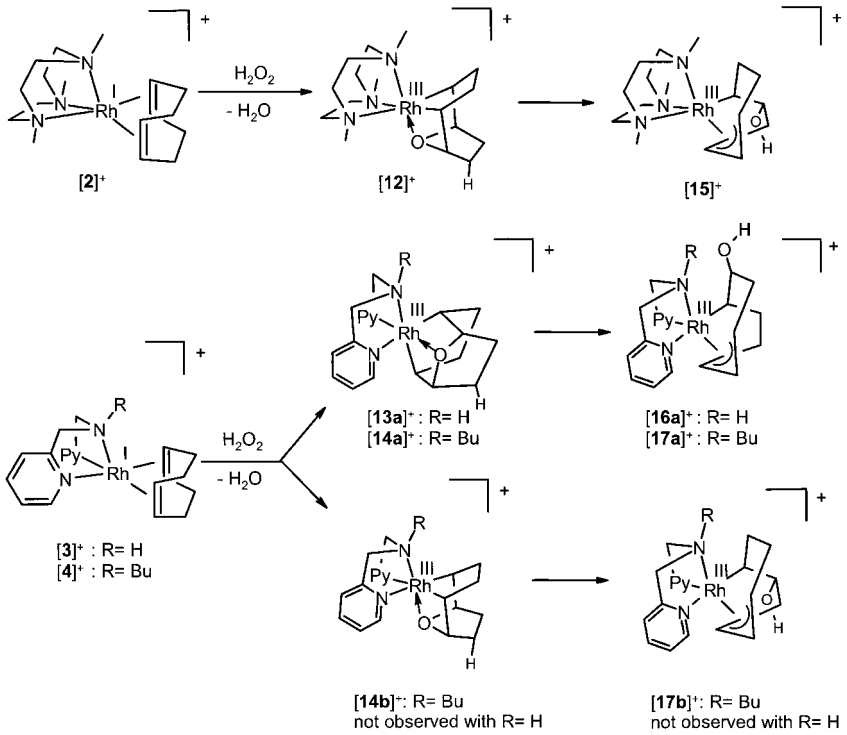

Scheme 4. Selective oxidation of Rh^{I}(cod) complexes by H_2O_2; formation of Rh^{III}-oxabicyclo-nonadiyl complexes and their rearrangement to Rh^{III}-hydroxycyclooctenediyl complexes.

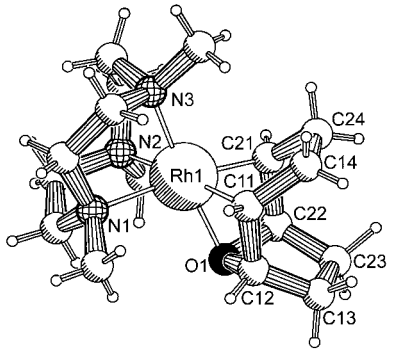

Figure 7. X-ray structure of oxabicyclononadiyl complex $[\mathbf{12}]^+$.

precipitation of $[\mathbf{13a}]BPh_4$. The structure of $[\mathbf{13a}]^+$ was derived from ^1H and ^{13}C NMR data.

The ^1H NMR spectrum obtained upon addition of H_2O_2 to $[\mathbf{4}]PF_6$ in $[D_6]$acetone at room temperature indicated the presence of two isomeric oxabicyclononadiyl complexes $[\mathbf{14a}]PF_6$ (asymmetric) and $[\mathbf{14b}]PF_6$ (symmetric), in a molar ratio 5:1.[22] Selective formation of asymmetric $[\mathbf{14a}]^+$ was observed when the reaction was carried out at $-10\,^{\circ}C$. We observed no isomerisation of $[\mathbf{14a}]^+$ to $[\mathbf{14b}]^+$ (or visa versa) at room temperature in $[D_6]$acetone. The formation of isomers $[\mathbf{14a}]^+$ and $[\mathbf{14b}]^+$ upon oxidation of $[\mathbf{4}]^+$ probably results from H_2O_2 attack at stereoisomeric five-coordinate species (e.g., the trigonal bipyramidal and square pyramidal isomers of Scheme 3). Apparently, the preference for oxidation of one specific stereoisomer is higher for $[\mathbf{3}]^+$ than for $[\mathbf{4}]^+$.

^1H NMR and FAB-MS spectra indicate that oxidation of complex $[\mathbf{5}]PF_6$ by H_2O_2 is analogous to that of $[\mathbf{4}]PF_6$. At room temperature a 1:5 mixture of the analogues of $[\mathbf{14a}]^+$ and $[\mathbf{14b}]^+$ is formed, whereas at $-10\,^{\circ}C$ only the analogue of $[\mathbf{14b}]^+$ is formed. ^1H NMR spectroscopy shows that instantaneous oxidation of the dinuclear complex $[\mathbf{8}][PF_6]_2$ in CD_3CN by H_2O_2 results in a mixture of three isomers; one containing two symmetric rhodium(III)oxabicyclononadiyl sites, one containing a symmetric and an asymmetric site, and one containing two asymmetric sites.

In contrast to the instantaneous, selective, oxidation of complexes $[\mathbf{2}]^+$, $[\mathbf{3}]^+$, $[\mathbf{4}]^+$, $[\mathbf{5}]^+$ and $[\mathbf{8}]^{2+}$, oxidation of the sterically hindered complexes $[\mathbf{6}]^+$ and $[\mathbf{7}]^+$ (see Scheme 1) with H_2O_2 is very slow and nonselective. In the presence of a tenfold excess of H_2O_2, solutions of both $[\mathbf{6}]^+$ and $[\mathbf{7}]^+$ proved stable for at least two hours. After 20 hours, ^1H NMR spectroscopy indicated the formation of a complex mixture of reaction products. The methylgroups at the pridine 6-position apparently prevent attack of H_2O_2 at the rhodium(I) centre.

The obtained oxabicyclononadiyl complexes $[\mathbf{12}]PF_6$ and $[\mathbf{14a}]^+/[\mathbf{14b}]PF_6$ are stable at room temperature. However, at this temperature the analogous complex $[\mathbf{13a}]BPh_4$ slowly converts to the 2-hydroxycycloocta-4-ene-1,6-di-yl (hydroxycyclooctenediyl) complex $[\mathbf{16a}]BPh_4$, both in solution and in the solid state (Scheme 4). The hydroxycyclooctenediyl fragment contains a 2-hydroxyalkyl and a η^3-allyl moiety. The structure of $[\mathbf{16a}]^+$ has been determined by single-crystal X-ray crystallography (Figure 8). The solution structure, as determined by ^1H NMR and ^{13}C NMR, and ^1H NOESY, ^1H COSY and $^1H-^{13}C$ correlation techniques, is in accordance with the X-ray structure.

The rearrangement of $[\mathbf{13a}]^+$ to $[\mathbf{16a}]^+$ is accelerated by acid, as observed in ^1H NMR spectroscopy. In the absence of added acid, conversion in CD_2Cl_2 at room temperature

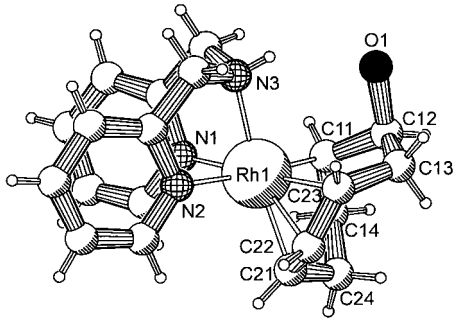

Figure 8. X-ray structure of hydroxycyclooctenediyl complex $[\mathbf{16a}]^+$.

proceeds to approximately 1% in two hours, whereas in the presence of 0.2 equivalents of the noncoordinating acid $[H(OEt_2)_2]B(C_6H_3(CF_3)_2)_4$ ($HBAr^f_4$)[23] conversion is quantitative within two hours.

The observed N(3)–O(1) distance of 3.007 Å in the X-ray structure of $[\mathbf{16a}]^+$ (Figure 8) is indicative for the presence of a N-H···O hydrogen bridge.[24] The selective formation of $[\mathbf{16a}]^+$ from $[\mathbf{13a}]^+$ might have been controlled by the formation of this hydrogen bridge. However, heating of the analogous $[\mathbf{14a}]PF_6$ (obtained by oxidation of $[\mathbf{4}]^+$ at $-10\,^\circ C$) in CD_3CN at $80\,^\circ C$ for 12 hours results in the selective formation of hydroxycyclooctenediyl complex $[\mathbf{17a}]PF_6$, according to ^1H NMR and ^1H NOESY spectra. This implies that the hydrogen bridge in $[\mathbf{16a}]^+$ is not responsible for the observed selectivity. Heating a 5:1 mixture of $[\mathbf{14a}]PF_6$ and $[\mathbf{14b}]PF_6$ (obtained by oxidation of $[\mathbf{4}]^+$ at room temperature) in CD_3CN results in a 5:1 ratio of $[\mathbf{17a}]^+$ and a second complex, which according to ^1H NMR is isomer $[\mathbf{17b}]^+$ (Scheme 4). Likewise, oxabicyclononadiyl complex $[\mathbf{12}]X$ ($X^- = PF_6^-/BPh_4^-$) rearranges upon heating in CH_3CN to hydroxycyclooctenediyl complex $[\mathbf{15}]X$ (Scheme 4). Complex $[\mathbf{15}]PF_6$ was isolated in quantitative yield by evaporation of the solvent. The structure of $[\mathbf{15}]PF_6$ has been determined by X-ray crystallography (see Figure 9). The structure showed

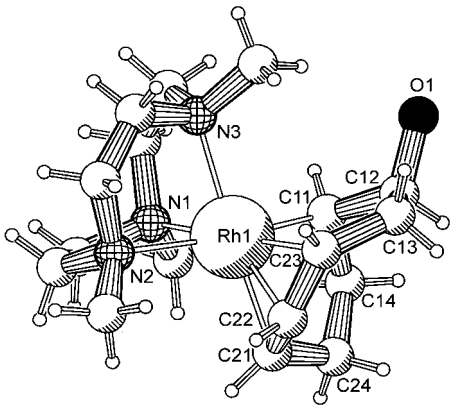

Figure 9. X-ray structure of hydroxycyclooctenediyl complex $[\mathbf{15^A}]^+$ (same orientation as $[\mathbf{16\ a}]^+$).

disorder, which could adequately be refined as a superposition of two cations $[\mathbf{15^A}]^+$ and $[\mathbf{15^B}]^+$. The solution structure of $[\mathbf{15}]^+$, as determined by ^1H NMR and ^{13}C NMR spectroscopy, and ^1H NOESY, ^1H COSY and $^1H-^{13}C$ correlation techniques, is in accordance with the X-ray structure.

The coordination geometry of the rhodium atoms in $[\mathbf{16a}]^+$ and $[\mathbf{15^A}]^+/[\mathbf{15^B}]^+$ is pseudooctahedral and very similar to that of $[(P_3O_9)Ir^{III}(2\text{-hydroxycycloocta-4-ene-1,6-di-yl})]^{2-}$ reported by Klemperer et al.[7] Selected bond lengths and angles are summarised in Tables 1 and 2. In both complexes the η^3-allyl fragment is symmetrically coordinated. In $[\mathbf{16a}]^+$ the Rh–N2 distance is longer than the Rh–N1 and Rh–N3 distances, reflecting the larger *trans* influence of the β-hydroxy-alkyl fragment relative to the allyl fragment. A similar difference is observed for the Ir–O distances in $[(P_3O_9)Ir^{III}(2\text{-hydroxycycloocta-4-ene-1,6-di-yl})]^{2-}$.

In contrast to the oxidation of $[\mathbf{2}]PF_6$, oxidation of complex $[\mathbf{1}]PF_6$ in CD_3CN at room tempreature with aqueous H_2O_2 proceeds directly to a hydroxycyclooctenediyl complex in 70% selectivity (according to ^1H NMR spectroscopy; 30% unidentified products) without detectable formation of an oxabicyclononadiyl intermediate. Oxidation of four-coordinate $[\mathbf{9}]PF_6$ by aqueous H_2O_2 in $[D_6]$acetone at room temperature also results in direct formation of the hydroxycyclooctenediyl complex. The selectivity in this case is 100%, as was concluded from ^1H NMR spectroscopy.[25]

Attempts to oxidise the hed complexes $[\mathbf{10}]^+$ and $[\mathbf{11}]^+$ (Scheme 2) by aqueous H_2O_2 in various solvents (acetone, CH_3CN or CH_2Cl_2) resulted in elimination of hed. For both $[\mathbf{10}]^+$ and $[\mathbf{11}]^+$ this reaction is accompanied by evolution of gas. This seems to indicate rhodium-catalysed disproportionation of H_2O_2 into H_2O and O_2 (catalase activity). Such H_2O_2 decomposition was not observed in reaction of H_2O_2 with any of the cod complexes. The reaction of H_2O_2 with $[\mathbf{11}]^+$ was much slower than with $[\mathbf{10}]^+$, probably because the methyl groups at the pyridine 6-position in $[\mathbf{11}]^+$ hamper attack of H_2O_2 at the rhodium(I) centre (Scheme 2).

Oxidation by O_2 (air): In the absence of added acid, none of the above cod complexes reacts with O_2. In the presence of $HBAr^f_4$, some of them are oxidised by O_2 (air) to the same products as obtained by oxidation with H_2O_2 (Scheme 4). The selectivities in oxidation by O_2 proved to be critically dependent on the nitrogen-donor ligand and the solvent. Table 4 summarises the results.

Selective oxidation of the cod fragment by O_2 is only observed for $[\mathbf{3}]^+$ in CH_2Cl_2. It results in formation of the hydroxycyclooctenediyl complex $[\mathbf{16a}]^+$. In the same solvent, complex $[\mathbf{1}]^+$ is oxidised to $[(Cn)Rh^{III}(\text{hydroxycyclooctenediyl})]^+$ in only 70% selectivity. Oxidation of complex $[\mathbf{4}]^+$ in CH_2Cl_2 results in consumption of the added H^+ under elimination of cod. The clear differences between BPA complex $[\mathbf{3}]^+$ and BuBPA complex $[\mathbf{4}]^+$ upon oxidation in CH_2Cl_2, disappear upon oxidation in CH_3CN; for both complexes 50% of the cod dissociates and 50% is oxidised.

Table 4. Conditions and results of oxidation of Rh^I(cod) complexes by O_2.

		Solvent	Acid (equiv)	Conv. [%]	Oxabicyclo-nonadiyl [%]	Hydroxycyclo-octenediyl [%]	Free COD [%]	Unknown [%]
$[\mathbf{1}]PF_6$	Cn	CH_2Cl_2	$HBAr^f_4$ (0.2)	100	–	70	–	30
$[\mathbf{3}]PF_6$	BPA	CH_2Cl_2	$HBAr^f_4$ (0.2)	100	–	100[a]	–	–
$[\mathbf{4}]PF_6$	BuBPA	CH_2Cl_2	$HBAr^f_4$ (0.3)	30	–	–	30	–
$[\mathbf{3}]PF_6$	BPA	CH_3CN	–	100	–	50[a]	50	–
$[\mathbf{4}]PF_6$	BuBPA	CH_3CN	NH_4PF_6 (0.2)	100	50[b]	–	50	–

All experiments under 1.6 bar O_2. Percentages conversion and yield are based on ^1H NMR integral ratios [a] $[\mathbf{16a}]^+$. [b] 40% $[\mathbf{14a}]^+$ and 10% $[\mathbf{14b}]^+$.

0947-6539/99/0510-2928 $ 17.50+.50/0 *Chem. Eur. J.* **1999**, *5*, No. 10

Upon treatment of $[\mathbf{2}]^+$ with $[H(OEt_2)_2]BF_4$ and O_2 in CH_2Cl_2, the peaks in the ^1H NMR spectrum shift, but oxidation of the cod fragment is not observed. Like BuBPA complex $[\mathbf{4}]^+$, BuBLA complex $[\mathbf{6}]^+$ reacts stoichiometrically with O_2 and $HBAr^f_4$ in CH_2Cl_2 under dissociation of cod. Exposure of the hed complexes $[\mathbf{10}]PF_6$ or $[\mathbf{11}]PF_6$ to O_2 or air leads to slow dissociation of hed, similar to that in the reaction of these complexes with H_2O_2.

We investigated the oxidation of $[\mathbf{3}]^+$ by O_2 in more detail. As indicated by ^1H NMR spectroscopy, exposure of a CD_2Cl_2 solution of $[\mathbf{3}]PF_6$ at room temperature to air or O_2 results in the slow formation of a mixture of $[\mathbf{13a}]PF_6$ and $[\mathbf{16a}]PF_6$ (Scheme 4), which subsequently converts to $[\mathbf{16a}]PF_6$ in four days. From this reaction mixture we isolated pure $[\mathbf{16a}]PF_6$ in 90% yield. Under these conditions a CD_2Cl_2 solution of $[\mathbf{3}]BPh_4$ proved to be stable. Apparently, oxidation of $[\mathbf{3}]^+$ is mediated by traces of acid (e.g., NH_4PF_6) that are scavenged by reaction with BPh_4^-.[26]

The oxidation rate of $[\mathbf{3}]^+$ under 1.6 bar of O_2 as a function of added $HBAr^f_4$ was followed by ^1H NMR spectroscopy (Figure 10). The plots of $\ln[A_t/A_0]$ versus time result in

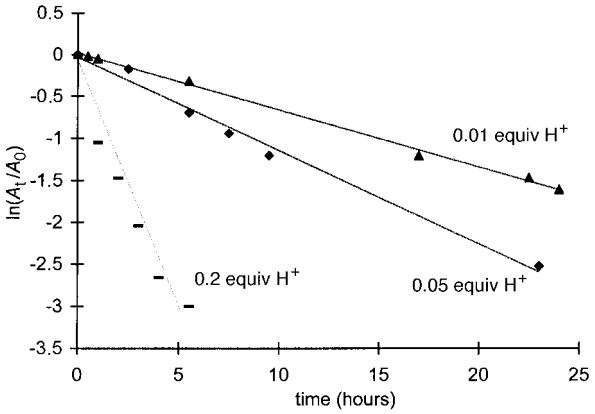

Figure 10. Plot of $\ln(A_t/A_0)$ versus time in the oxidation of $[\mathbf{3}]^+$ by O_2; the figure indicates first-order kinetics in $[\mathbf{3}]^+$ and the influence of added $HBAr^f_4$ on the reaction rate.

straight lines that are characteristic for first-order kinetics in $[\mathbf{3}]^+$ (A_t = concn $[\mathbf{3}]^+$ at time t, A_0 = initial concn $[\mathbf{3}]^+$).[27] Clearly the oxidation rate increases with the amount of $HBAr^f_4$ added (Figure 10). Upon addition of >0.05 equivalents of $HBAr^f_4$, only minor amounts of $[\mathbf{13a}]^+$ were detectable during the reaction of $[\mathbf{3}]^+$ to $[\mathbf{16a}]^+$. This is consistent with our previous observation that the transformation of $[\mathbf{13a}]^+$ to $[\mathbf{16a}]^+$ is acid-catalysed (see above).

Addition of one equivalent $HBAr^f_4$ to $[\mathbf{3}]PF_6$ in CD_2Cl_2 under N_2 results in broadening of the pyridyl signals at room temperature. At $-48\,^\circ C$ the square-planar dicationic (pyridinium-amine-pyridine)Rh^I(cod) complex $[\mathbf{18}]^{2+}$ can be identified from ^1H and ^{13}C NMR spectra (Scheme 5).[28] Exposure of the resulting solution to O_2 at room temperature results in quantitative conversion to $[\mathbf{16a}]^+$ within one hour.

Addition of equimolar amounts of a radical-trapping compound such as ethanol or 2-*tert*-butyl-4-methylphenol[29] had no effect on the oxidation of $[\mathbf{3}]^+$ by O_2. Reaction of $[\mathbf{3}]PF_6$ with O_2 in CH_2Cl_2 in the presence of approximately 50 equivalents of $H_2{}^{18}O$ showed no significant incorporation of ^{18}O in the final product $[\mathbf{16a}]^+$. Volumetric gas burette measurements for the reaction of $[\mathbf{3}]^+$ with O_2 indicated a consumption of one mole of O_2 per mole of $[\mathbf{3}]^+$.

Discussion

2-Rhodaoxetane rearrangement: It seems reasonable to assume that oxidation of Rh^I-cod to Rh^{III}-oxabicyclononadiyl proceeds via an intermediate 2-rhoda(III)oxetane that subsequently undergoes insertion of the second double bond of cod into the Rh^{III}–O bond (Scheme 6). An analogous trimethaphosphate-2-irida(III)oxetane has been isolated from the reaction of dioxygen with $[(P_3O_9)Ir^I(cod)]^{2-}$.[7] For this 2-iridaoxetane, insertion of the second double bond of cod into the Ir–O bond was not observed.

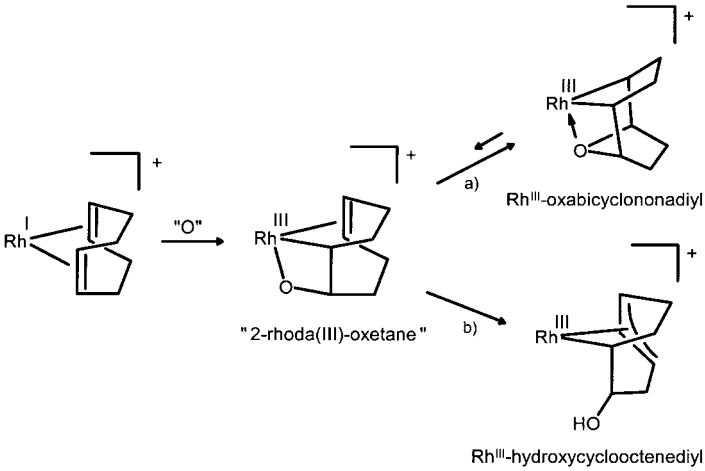

Scheme 6. a) Formation of Rh^{III}-oxabicyclononadiyl by olefin insertion into the Rh–O bond of a 2-rhoda(III)oxetane intermediate. b) Rearrangement to Rh^{III}-hydroxycyclooctenediyl via abstraction of an allylic hydrogen.

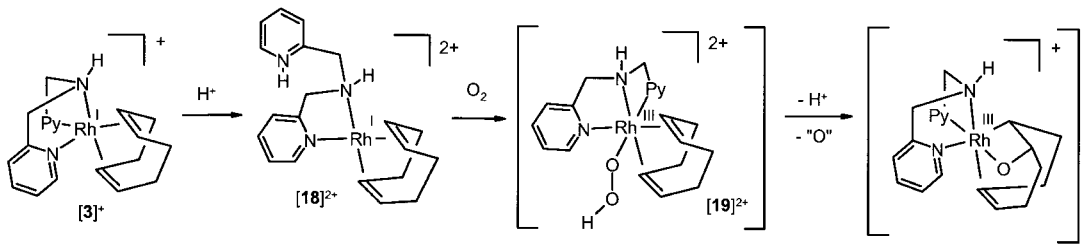

Scheme 5. Protonation of $[\mathbf{3}]^+$ to $[\mathbf{18}]^{2+}$. Oxidation of $[\mathbf{3}]^+$ via proposed hydroperoxo intermediate $[\mathbf{19}]^{2+}$.

We propose that rearrangement of the oxabicyclononadiyl fragment to the hydroxycyclooctenediyl fragment proceeds via formation of the intermediate 2-rhoda(III)oxetane and net abstraction of an allylic proton by the nucleophilic oxygen of the 2-rhodaoxetane (Scheme 6). This would be similar to the rearrangement observed for the above mentioned 2-iridaoxetane.[7] We cannot exclude that the hydroxycyclooctenediyl fragment is formed directly from the oxabicyclononadiyl fragment by an elimination reaction, but the route via a 2-rhodaoxetane seems more feasible. The faster rearrangement of [**13a**]$^+$ to [**16a**]$^+$ in the presence of acid could well be the result of protonation of the 2-rhodaoxetane oxygen. Subsequent electrophilic attack of the Rh^{III} centre at the allylic C–H bond would thus complete acid-catalysed formation of [**16a**]$^+$.

Mechanism of oxygenation by H_2O_2: The relative stability of [**6**]$^+$ and [**7**]$^+$ towards H_2O_2 suggest that the bulky Py-Me donors prevent H_2O_2 attack at rhodium(I). The nature of the oxidation products also suggests a mechanism involving O transfer via rhodium (O transfer through *endo* attack of "O" at cod double bond). Direct O transfer to the olefin would have resulted in *exo* attack, as in the Wacker oxidation of Pd–olefin complexes.[30] One could imagine a mechanism involving electrophilic attack at Rh^I by H_2O_2, resulting in transfer of OH^+ to Rh^I.[31] Insertion of a cod double bond into the thus obtained Rh^{III}–OH bond and abstraction of a proton from the resulting 2-hydroxyalkyl fragment would provide the 2-rhodaoxetane intermediate. However, alternative mechanisms, such as O transfer from H_2O_2[32] to Rh^I can not be excluded.

Mechanism of oxygenation by O_2: The reaction of the dianionic Ir^I complex $[(P_3O_9)Ir^I(cod)]^{2-}$ with O_2, reported by Klemperer et al,[7] is to our knowledge the only previous example of the oxidation of a metal–cod complex to a metal–hydroxycyclooctenediyl complex. This reaction was proposed to proceed through the dinuclear activation of O_2 in an [Ir]-O-O-[Ir] intermediate on the basis of volumetric gas burette measurements; these indicated consumption of 0.5 moles of O_2 per mole of $[(P_3O_9)Ir^I(cod)]^{2-}$.

With Klemperer's dinuclear mechanism in mind, we designed the dinuclear complex [**8**]$^{2+}$. We argued that, for reasons of entropy, dinuclear complex [**8**]$^{2+}$ might be more prone to oxidation by O_2 than its mononuclear analogue [**4**]$^+$ (or [**3**]$^+$).[33] However, we observed no differences between [**8**]$^{2+}$ and [**4**]$^+$ in the rate of reaction with O_2. We have observed selective oxidation only for the mononuclear BPA-complex [**3**]$^+$ in CH_2Cl_2. In contrast to the O_2 uptake reported for $[(P_3O_9)Ir^I(cod)]^{2-}$, our volumetric gas burette measurements for the reaction of [**3**]$^+$ with O_2 indicate consumption of one mole of O_2 per mole of [**3**]$^+$.

As the reaction of [**3**]$^+$ with O_2 in the presence of approximately 50 equivalents of $H_2{}^{18}O$ showed no significant incorporation of ^{18}O-labeled oxygen in the final product [**16a**]$^+$, the oxygen atom in oxygenation of [**3**]$^+$ must stem from O_2. Therefore a mechanism involving nucleophilic attack of H_2O (Wacker-type mechanism) on an initially formed $[Rh^{III}(cod)]^{3+}$ fragment can be excluded.

The reaction of [**3**]$^+$ with O_2 is clearly catalysed by H^+. The kinetic data suggest that the reaction proceeds via a mononuclear complex in the rate-determining step. It is tempting to propose that [**3**]$^+$, O_2 and H^+ form the hydroperoxo complex $[(BPA)Rh^{III}(OOH)(cod)]^{2+}$ [**19**]$^{2+}$ as the initial oxidation product from the reaction of [**18**]$^{2+}$ with O_2 (Scheme 5). Precedents for this type of reaction have been reported for a similar $'N_3'Rh^I$(diphos) complex.[34] The observed dissociation of cod (vide supra) in the reaction of [**3**]PF_6 with O_2 in CH_3CN could be the result of substitution of cod in [**19**]$^{2+}$ by CH_3CN.

In view of the observed consumption of one mole of O_2 per mole of [**3**]$^+$, the hydroperoxo intermediate [**19**]$^{2+}$ must lose one oxygen atom in formation of a 2-rhodaoxetane. The fate of this oxygen atom is presently obscure. Other mechanisms, for example, involving one-electron oxidation of Rh^I to Rh^{II} by O_2 cannot be ruled out completely. However, the observation that a radical-trapping compound such as 2-*tert*-butyl-4-methylphenol has no influence on the oxidation of [**3**]$^+$ by O_2 indicates a nonradical pathway.

Experimental section

General methods: All procedures were performed under N_2 with standard schlenk techniques unless indicated otherwise. Solvents (p.a.) were deoxygenated by bubbling through a stream of N_2 or by the freeze-pump-thaw method. The temperature indication room temperature (RT) corresponds to about 20 °C. NMR experiments were carried out on a Bruker DPX200 (200 MHz and 50 MHz for ^1H and ^{13}C, respectively), a Bruker AC300 (300 MHz and 75 MHz for ^1H and ^{13}C, respectively) and a Bruker WM400 (400 MHz and 100 MHz for ^1H and ^{13}C, respectively). Solvent shift reference for ^1H NMR: [D_6]acetone $\delta_H = 2.05$, CD_3CN $\delta_H = 1.98$, CD_2Cl_2 $\delta_H = 5.31$, [D_6]DMSO $\delta_H = 2.50$. For ^{13}C NMR: [D_6]acetone $\delta_C = 29.50$, CD_3CN $\delta_C = 1.28$, CD_2Cl_2 $\delta_C = 54.20$, [D_6]DMSO $\delta_c = 39.50$. Abbreviations used are s = singlet, d = doublet, dd = doublet of doublets, ddd = doublet of doublets of doublets, t = triplet, dt = doublet of triplets, q = quartet, dq = doublet of quartets, m = multiplet and br = broad. Elemental analysis (C,H,N) were carried out on a Carlo Erba NCSO analyser. Mass Spectra (EI, FAB) were recorded on a VG 7070 mass spectrometer or on a JEOL JMS SX/SX102A four sector mass spectrometer (NBA = 3-nitrobenzyl alcohol). Cyclic voltammetry measurements were performed with an Eco Chemie Autolab PGSTAT20. A conventional three-electrode cell, with Pt working and auxiliary electrodes and 0.1 M $[(n\text{Bu})_4\text{N}]PF_6$ (TBAH) electrolyte was used. An Ag/AgI reference electrode (grain of AgI, 0.02 M $[(n\text{Bu})_4\text{N}]$I (TBAI) and 0.1 M TBAH) was employed. The ligand TPBN was prepared according to a literature procedure.[35] 1,4,7-trimethyl-1,4,7-triazacyclononane (Cn*) was generously supplied by Unilever Research. [{(cod)Rh(μ-Cl)}$_2$]and [{(hed)Rh(μ-Cl)}$_2$] were prepared according to literature procedures.[36] All other chemicals are commercially available and were used without further purification, unless stated otherwise.

X-ray diffraction: Crystals of [**2**]BPh_4 and [**12**]PF_6 were obtained from methanol by slow evaporation (RT) of the solvent. Crystals of [**3**]BPh_4 and [**16a**]BPh_4 suitable for X-ray diffraction studies were obtained from CH_3CN by slow cooling of a hot, saturated solution. Crystals of [**6**]PF_6 and [**7**]$PF_6 \cdot$ acetone suitable for X-ray diffraction studies were obtained from acetone by slowly cooling a saturated solution at RT to −20 °C. Crystals of [**8**][PF_6]$_2$ were obtained by slow diffusion of Et_2O into a CH_3CN solution. Crystals of [**15**]PF_6 were obtained from acetone by slow evaporation (RT) of the solvent.

The structures were solved by the program system DIRDIF[37] by using the program PATTY[38] to locate the heavy atoms. Unit-cell dimensions were determined from the angular setting of 25 reflections for [**2**]BPh_4, [**6**]PF_6, [**8**][PF_6]$_2$, [**15**]PF_6 and [**16a**]BPh_4, 15 reflections for [**3**]BPh_4, 9 reflections for [**12**]PF_6 and 7 reflections for [**7**]$PF_6 \cdot$ acetone. Intensity data were corrected for Lorentz and polarisation effects. For all structures except for

0947-6539/99/0510-2930 $ 17.50+.50/0 *Chem. Eur. J.* **1999**, *5*, No. 10

[**3**]BPh_4, semiempirical absorption correction (ψ-scan)[39] was applied. The structures were refined with standard methods (refinement against F^2 of all reflections with SHELXL 97[40]) with anisotropic parameters for the nonhydrogen atoms. All hydrogen atoms were placed at calculated positions. For [**2**]BPh_4, [**12**]PF_6 and [**16a**]BPh_4 the hydrogen atoms were subsequently freely refined. Selected bond lengths an angles are summarised in Tables 1 and 2. Other relevant crystal data are summarised in Table 5. Drawings were generated with the program PLATON.[41]

*Complex [**8**][PF_6]$_2$*: The PF_6^- ion was threefold disordered about one F-P-F axis. The P–F and F–F bonds were restrained to target values with an estimated standard deviation of 0.03. The occupation factors of the disordered fluorine atoms were also refined.

*Complex [**16a**]BPh_4*: The hydrogens attached to atoms N3, C11, C12, C21, C22 and C24 were taken from a difference Fourier map and were freely refined subsequently. The hydrogen attached to atom O1 could not be localised and is therefore not included in the model. All other hydrogens were placed at calculated positions and were refined riding on the parent atoms.

Crystallographic data (excluding structure factors) for the structures reported in this paper have been deposited with the Cambridge Crystallographic Data Centre as supplementary publication no. CCDC-14725 ([**2**]BPh_4), 114726 ([**3**]BPh_4), 114727 ([**6**]PF_6), 114728 ([**7**]PF_6.acetone), 114729 ([**8**][PF_6]$_2$), 114730 ([**12**]PF_6), 114731 ([**16a**]BPh_4), and 114732 ([**15**]PF_6). Copies of the data can be obtained free of charge on application to CCDC, 12 Union Road, Cambridge CB2 1EZ, UK (fax: (+44) 1223-336-033; e-mail: deposit@ccdc.cam.ac.uk).

Synthesis

***N*-Benzyl-*N*,*N*-di(2-pyridylmethyl)amine (BzBPA) and *N*-butyl-*N*,*N*-di(2-pyridylmethyl)amine (BuBPA)**: The ligands BzBPA and BuBPA were prepared by procedures similar to that reported for TPEN,[35] by using benzylamine and *n*-butylamine, respectively, instead of 1,4-diaminobutane. For both BzBPA and BuBPA, the crude product, obtained as a brown oil, was purified by column chromatography (silica 60 H; CH_3Cl/MeOH 100:10 v:v). The isolated products (red-brown, viscous oils) were pure according to ^{1}H NMR spectroscopy.

BzBPA: ^{1}H NMR (200.13 MHz, $CDCl_3$, 298 K): $\delta = 8.48$ (d, ^3J(H,H) = 4.7 Hz, 2 H; Py-H6), 7.60–7.05 (m, 11 H; Py-H4, Py-H3, Py-H5, Ph), 3.80 (s, 4 H; N-CH_2-Py), 3.67 (s, 2 H; N-CH_2-Ph); ^{13}C NMR {^{1}H} (50.32 MHz, $CDCl_3$, 298 K): $\delta = 160.07$ (Py-C2), 149.37 (Py-C6), 139.23 (Ph-C1), 136.87 (Py-C4), 129.27 (Ph-C2), 128.75 (Ph-C3), 127.50 (Ph-C4), 123.20 (Py-C3), 122.39 (Py-C5), 60.35 (N-CH_2-Py), 58.88 (N-CH_2-Ph).

BuBPA: ^{1}H NMR (200.13 MHz, $CDCl_3$, 298 K): $\delta = 8.57$ (d, ^3J(H,H) = 4.7 Hz, 2 H; Py-H6), 7.66–7.00 (m, 6 H; Py-H4, Py-H3, Py-H5), 3.87 (s, 4 H; N-CH_2-Py), 2.60 (t, ^3J(H,H) = 7.2 Hz, 2 H; N-CH_2-C_3H_7), 1.58 (m, 2 H; N-CH_2-CH_2-C_2H_5), 1.35 (m, 2 H; N-C_2H_4-CH_2-CH_3), 0.89 (t, ^3J(H,H) = 7.2 Hz, 3 H; N-C_3H_6-CH_3); EI-MS: *m*/*z* (%): 255 (1.3) $[M]^+$, 212 (3.28) $[M - C_3H_7]^+$, 198 (0.95) $[M - C_4H_9]^+$, 163 (100.0) $[M - CH_2Ph]^+$, 93 (45.2) $[CH_2Py+H]^+$.

***N*-Benzyl-*N*,*N*-di[(6-methyl-2-pyridylmethyl)]amine (BzBLA)**: 2-Chloromethyl-6-methylpyridine hydrochloride[42] (1.50 g, 8.5 mmol), benzylamine (0.43 g, 4.01 mmol) and (12 g, 140 mmol) Na_2CO_3 dissolved in water (10 mL) were added to CH_3CN (100 mL). The resulting suspension was heated to reflux for 16 hours. The mixture was filtered, and the filtrate was evaporated to yield a yellow oil, to which Et_2O (100 mL) was added. Partial evaporation of the solvent resulted in precipitation of BzBLA as a white solid, which was recrystallised as a white crystals from a saturated hexane solution at −20 °C. Yield 36% (0.44 g, 1.39 mmol); m.p. 76.9 °C; ^{1}H NMR (200.13 MHz, $CDCl_3$, 298 K): $\delta = 7.62–7.00$ (m, 11 H; Py-H4, Py-H3, Py-H5, Ph-H), 3.86 (s, 4 H; N-CH_2-Py), 3.75 (s, 2 H; N-CH_2-Ph), 2.54 (s, 6 H; Py-CH_3); ^{13}C {^{1}H} (75.47 MHz, [D_6]acetone, 298 K): $\delta = 160.4$ (Py-C2), 158.5 (Py-C6), 140.6 (Ph-C1), 137.7 (Py-C4), 130.0 (Ph-C2,Ph-C3), 128.1 (Ph-C4), 122.3 (Py-C5), 120.6 (Py-C3), 61.0 (N-CH_2-Ph), 59.3 (N-CH_2-Ph),

Table 5. Crystallographic data for [**2**]BPh_4, [**3**]BPh_4, [**6**]PF_6, [**7**]PF_6.(acetone), [**8**][PF_6]$_2$, [**12**]PF_6, [**15**]PF_6 and [**16a**]BPh_4.

	[**2**]BPh_4	[**3**]BPh_4	[**6**]PF_6	[**7**]PF_6.(acetone)
formula	$C_{41}H_{53}N_3BRh$	$C_{44}H_{45}N_3BRh$	$C_{26}H_{37}N_3RhPF_6$	$C_{32}H_{41}N_3ORhPF_6$
crystal size [mm]	0.18 × 0.17 × 0.09	0.38 × 0.32 × 0.17	0.44 × 0.18 × 0.17	0.24 × 0.17 × 0.13
M_w	701.58	729.55	639.47	731.56
T [K]	208(2)	293(2)	208(2)	208(2)
crystal system	monoclinic	monoclinic	monoclinic	monoclinic
space group	$P2_1/n$	$P2_1/c$	$P2_1/n$	$P2_1$
a [Å]	10.5435(4)	13.6402(8)	16.0922(3)	10.4858(11)
b [Å]	21.4531(8)	13.9322(11)	17.6350(4)	25.150(10)
c [Å]	15.5482(6)	19.017(4)	18.9795(4)	12.094(10)
α [°]	90	90	90	90
β [°]	92.233(3)	100.125(7)	94.5930(17)	100.931(10)
γ [°]	90	90	90	90
V [Å^3]	3514.2(2)	3557.7(8)	5368.8(2)	3132(3)
ρ_{calcd} [g cm^{-3}]	1.326	1.362	1.582	1.552
Z	4	4	8	4
diffractometer (scan)	Enraf-Nonius CAD4 (θ-2θ)	Enraf-Nonius CAD4 (θ-2θ)	Enraf-Nonius CAD4 (θ-2θ)	Enraf-Nonius CAD4 (ω)
Radiation	$Cu_{K\alpha}$	$Cu_{K\alpha}$	$Cu_{K\alpha}$	$Cu_{K\alpha}$
λ [Å]	1.54184	1.54184	1.54184	1.54184
F(000)	1480	1520	2624	1504
θ range [°]	3.51 to 69.96	3.29 to 69.97	3.43 to 69.96	3.51 to 70.18
index ranges	$-12 \le h \le 12$ $0 \le k \le 26$ $0 \le l \le 18$	$-16 \le h \le 16$ $0 \le k \le 16$ $0 \le l \le 23$	$-19 \le h \le 0$ $-21 \le k \le 0$ $-23 \le l \le 23$	$-12 \le h \le 0$ $-30 \le k \le 0$ $-14 \le l \le 14$
range of relative transmission factors	0.887/1.141	–	0.904/1.125	0.968/1.043
measured reflections	6894	6948	10544	6420
unique reflections	6644	6731	10166	6080
observed refl. [$I_o > 2\sigma(I_o)$]	5415	6372	9506	5191
parameters	627	447	673	830
goodness-of-fit on F^2	1.030	1.118	1.059	1.051
R [$I_o > 2\sigma(I_o)$]	0.0350	0.0427	0.0660	0.0474
$wR2$ [all data]	0.0873	0.1112	0.1971	0.1271
ρ_{fin} (max/min) [e Å^{-3}]	1.002/−1.371	1.556/−1.330	1.258/−3.971	2.506/−0.769

Table 5. (Continued).

	[**8**][PF_6]$_2$	[**12**]PF_6	[**15**]PF_6	[**16a**]BPh_4
formula	$C_{44}H_{56}N_6Rh_2P_6F_{12}$	$C_{17}H_{33}N_3ORhPF_6$	$C_{17}H_{33}N_3ORhPF_6$	$C_{44}H_{45}N_3BORh$
crystal size [mm]	0.15 × 0.20 × 0.50	0.45 × 0.10 × 0.05	0.71 × 0.62 × 0.62	0.28 × 0.26 × 0.13
M_w	1164.71	543.34	543.34	745.55
T [K]	293(2)	150(2)	293(2)	208(2)
crystal system	triclinic	monoclinic	monoclinic	monoclinic
space group	$P\bar{1}$	$P2_1/c$	$P2_1/c$	$P2_1/c$
a [Å]	9.1097(8)	10.2472(10)	9.3418(2)	12.7629(4)
b [Å]	10.3543(13)	13.0331(8)	15.0175(7)	15.1669(9)
c [Å]	12.7799(12)	15.5345(8)	15.5792(5)	19.1220(5)
α [°]	87.247(12)	90	90	90
β [°]	70.953(10)	90.012(6)	92.450(2)	104.681(3)
γ [°]	89.428(15)	90	90	90
V [Å^3]	1138.1(2)	2074.7(3)	2183.61(14)	3580.6(3)
ρ_{calcd} [g cm^{-3}]	1.699	1.740	1.653	1.383
Z	1	4	4	4
diffractometer (scan)	Enraf-Nonius CAD4 (ω)	Nonius CAD4T rotating anode (ω)	Enraf-Nonius CAD4 (θ-2θ)	Enraf-Nonius CAD4 (θ-2θ)
Radiation	$Mo_{K\alpha}$	$Mo_{K\alpha}$	$Cu_{K\alpha}$	$Cu_{K\alpha}$
λ [Å]	0.71073	0.71073	1.54184	1.54184
F(000)	590	1112	1112	1552
θ range [°]	1.69 to 29.99	1.99 to 27.46	4.09 to 70.04	3.58 to 69.88
index ranges	$-12 \le h \le 10$ $-14 \le k \le 14$ $-17 \le l \le 17$	$0 \le h \le 13$ $-16 \le k \le 0$ $-20 \le l \le 20$	$0 \le h \le 11$ $-18 \le k \le 18$ $-18 \le l \le 18$	$-15 \le h \le 15$ $-18 \le k \le 0$ $-23 \le l \le 0$
range of relative transmission factors	0.970/1.051	0.973/1.025	0.826/1.327	0.869/1.216
measured reflections	12418	5204	8616	6997
unique reflections	6624	4761	4139	6781
observed refl. [$I_o > 2\sigma(I_o)$]	5573	3399	4023	6147
parameters	427	394	255	475
goodness-of-fit on F^2	1.045	1.026	1.048	1.029
R [$I_o > 2\sigma(I_o)$]	0.0380	0.0441	0.0709	0.0680
$wR2$ [all data]	0.0926	0.0915	0.1987	0.1723
ρ_{fin} (max/min) [e Å^{-3}]	0.905/ − 0.826	0.682/ − 0.662	1.701/ − 1.494	3.082/ − 3.053

24.8 (Py-*CH*$_3$); EI-MS: m/z (%): 317 (1.3) $[M]^+$, 226 (25.9) $[M - CH_2Ph]^+$, 211 (100.0) $[M - CH_2Ph - CH_3]^+$, 107 (78.2) $[CH_2PyCH_3]^+$; $C_{21}H_{23}N_3$ (317.43): calcd C 79.46, H 7.30, N 13.24; found C 79.26, H 7.29, N 13.02.

***N*-Butyl-*N*,*N*-di[(6-methyl-2-pyridylmethyl)]amine (BuBLA)**: The ligand BuBLA was prepared by a method similar to the synthesis of BzBLA from *n*-butylamine. The crude product, obtained as a brown oil, was purified by column chromatography (silica 60 H; CH_3Cl/MeOH 100:10 v:v). The isolated light brown powder was pure according to ^{1}H NMR spectrsocopy (Yield 33 %). ^{1}H NMR (200.13 MHz, $CDCl_3$, 298 K): $\delta = 7.54 - 7.00$ (m, 6 H; Py-H4, Py-H3, Py-H5), 3.82 (s, 4 H; N-*CH*$_2$-Py), 2.55 (t, ^3J(H,H) = 6.70 Hz, 2 H; N-*CH*$_2$-C_3H_7), 2.51 (s, 6 H; Py-*CH*$_3$), 1.53 (m, 2 H; N-CH_2-*CH*$_2$-C_2H_5), 1.31 (m, 2 H; N-C_2H_4-*CH*$_2$-CH_3), 0.83 (t, ^3J(H,H) = 7.21 Hz, 3 H; N-C_3H_6-*CH*$_3$).

(η^4-Cycloocta-1,5-diene)-(κ^3-1,4,7-triazacyclononane)rhodium(I)hexafluorophosphate ([1]PF_6): Cn (100 mg, 0.78 mmol) and [{(cod)Rh(μ-Cl)}$_2$] (192 mg, 0.39 mmol) were stirred in MeOH (25 mL) for 1 hour. Subsequently, NH_4PF_6 (350 mg, 2.15 mmol) was added. Partial evaporation of the solvent caused the precipitation of [**1**]PF_6 as a yellow powder, which was filtered and vacuum dried. Yield 75 % (284 mg); ^{1}H NMR (200.13 MHz, [D$_6$]acetone, 298 K): $\delta = 5.00$ (s, 3 H; NH), 3.44 (m, 4 H; −CH=CH−), 3.25 – 3.00 (m, 6 H; N-CH_2−), 2.95 – 2.65 (m, 6 H; N-CH_2−), 2.32 (m, 4 H; −C=C-CH_2-*exo*), 1.69 (m, 4 H; -C=C-CH_2-*endo*); ^{13}C{^{1}H} NMR (50.33 MHz, [D$_6$]acetone, 298 K): $\delta = 69.2$ (d, J(Rh,C) = 12.9 Hz; −CH=CH−), 48.7 (N-CH_2−), 31.7 (C=C−CH_2);. FAB-MS (NBA/CH_3CN): m/z: 340 $[M - PF_6]^+$, 825 $[2M - PF_6]^+$; $C_{14}H_{27}N_3RhPF_6$ (485.28): calcd C 34.65, H 5.61, N 8.66; found C 34.62, H 5.67, N 8.52.

(η^4-Cycloocta-1,5-diene)-(κ^3-1,4,7-trimethyl-1,4,7-triazacyclononane)rhodium(I)hexafluorophosphate/tetraphenylborate ([2]PF_6/BPh_4): Cn* (92 mg, 0.54 mmol) and [{(cod)Rh(μ-Cl)}$_2$] (134 mg, 0.27 mmol) were stirred in MeOH (25 mL) for 1 h. Subsequently, NH_4PF_6 (354 mg, 2.16 mmol) was added. Partial evaporation of the solvent caused the precipitation of [**2**]PF_6 as a yellow powder, which was filtered and vacuum dried. Yield 71 % (202 mg). By a similar procedure, using $NaBPh_4$ instead of NH_4PF_6, [**2**]BPh_4 was obtained. (NMR data given for [**2**]PF_6) ^{1}H NMR (200.13 MHz, [D$_6$]acetone, 298 K): $\delta = 3.56$ (m, 4 H; −CH=CH−), 3.1 – 2.85 (m, 12 H; N−CH_2−), 3.00 (s, 9 H; N−CH_3), 2.46 (m, 4 H; −C=C-CH_2-*exo*), 1.67 (m, 4 H; −C=C-CH_2-*endo*); ^{13}C{^{1}H} NMR (50.33 MHz, [D$_6$]acetone, 298 K): $\delta = 74.2$ (d, J(Rh,C) = 13.8 Hz; −CH=CH−), 58.4 (N-CH_2−), 51.2 (N-CH_3), 30.7 (C=C-*CH*$_2$). FAB-MS (NBA/CH_3CN): m/z: 382 $[M - PF_6]^+$, 909 $[2M - PF_6]^+$; $C_{17}H_{33}N_3RhPF_6$ (527.33): calcd C 38.72, H 6.31, N 7.97; found C 38.47, H 6.22, N 7.85; $C_{41}H_{53}N_3RhB$ (701.60): calcd C 70.19, H 7.61, N 5.99; found C 69.86, H 7.44, N 5.85.

(η^4-Cycloocta-1,5-diene)-[κ^3-fac-*N*,*N*-di(2-pyridylmethyl)amine]rhodium(I)-hexafluorophosphate/tetraphenylborate ([3]PF_6/BPh_4): Compounds [**3**]PF_6 and [**3**]BPh_4 were prepared by procedures similar to those described for [**2**]PF_6 and [**2**]BPh_4, but with the ligand BPA. (NMR data given for [**3**]BPh_4). ^{1}H NMR (200.13 MHz, CD_2Cl_2, 298 K): $\delta = 8.69$ (d, ^3J(H,H) = 5.4 Hz, 2 H; Py-H6), 7.51 (m, 2 H; Py-H4), 7.36 (m, 8 H; BAr-H2), 7.45 – 6.80 (m, 4 H; Py-H5, Py-H3), 7.01 (t,^3J(H,H) = 7.4 Hz, 8 H; BAr-H3), 6.86 (t, ^3J(H,H) = 7.4 Hz, 4 H; BAr-H4), 4.00 (dd[AB], ^2J(H,H) = 17.1 Hz, ^3J(NH,H) = 7.2 Hz, 2 H; N-CH_2-Py), 3.56 (m, 4 H; −CH=CH−), 3.32 (d[AB], ^2J(H,H) = 17.1 Hz, 2 H; N-CH_2-Py), 2.50 (m, 4 H; −C=C-CH_2-*exo*), 1.85 (m, 4 H; −C=C-CH_2-*endo*); ^{13}C{^{1}H} NMR (50.32 MHz, [D$_6$]DMSO, 298 K): $\delta = 163.4$ (q, ^1J(C,B) = 49.0 Hz; BAr-C1), 159.6 (Py-C2), 148.9 (Py-C6), 137.9 (Py-C4), 135.6 (BAr-C2), 125.4 (q, ^3J(C,B) = 2.8 Hz; BAr-C3), 124.0 (Py-C3), 122.5 (Py-C5), 121.6 (BAr-C4), 72.3 (d, J(Rh,C) = 13.0 Hz; −CH=CH−), 59.4 (N-CH_2-Py), 31.0 (C=C-CH_2); FAB-MS (NBA/CH_3CN): m/z: 410 $[M]^+$; $C_{20}H_{25}N_3RhPF_6$ (555.30): C 43.26, H 4.54, N 7.57; found C 42.86, H 4.29, 7.52; $C_{44}H_{45}N_3RhB$ (729.58): calcd C 72.44, H 6.22, N 5.76; found C 72.41, H 6.32, N 5.83.

(η^4-Cycloocta-1,5-diene)-[κ^3-*fac*-*N*-butyl-*N*,*N*-di(2-pyridylmethyl)amine]-rhodium(I)hexafluorophosphate ([4]PF_6): Compound [**4**]PF_6 was prepared by a procedure similar to that described for [**1**]PF_6, but with the ligand BuBPA. ^{1}H NMR (200.13 MHz, [D$_6$]acetone, 298 K): $\delta = 9.20$ (d, ^3J(H,H) = 5.4 Hz, 2 H; Py-H6), 7.74 (m, 2 H; Py-H4), 7.37 – 7.27 (m, 4 H; Py-H5, Py-H3), 4.62 (d[AB],^2J(H,H) = 16.3 Hz, 2 H; N-CH_2-Py), 4.25

0947-6539/99/0510-2932 $ 17.50+.50/0 *Chem. Eur. J.* **1999**, *5*, No. 10

(d[AB], ^2J(H,H) = 16.3 Hz, 2H; N-CH_2-Py), 4.06 (m, 2H; N-CH_2-CH_2-CH_2-CH_3), 3.83 (m, 4H; −CH=CH−), 2.65 (m, 4H; −C=C-CH_2-*exo*), 2.12 (m, 2H; N-CH_2-CH_2-CH_2-CH_3), 1.86 (m, 4H; −C=C-CH_2-*endo*), 1.59 (m, 2H; N-CH_2-CH_2-CH_2-CH_3), 1.09 (t, ^3J(H,H) = 7.4 Hz, 3H; N-CH_2-CH_2-CH_2-CH_3); $^{13}C\{^1H\}$ NMR (50.33 MHz, [D$_6$]acetone, 298 K): δ = 160.4 (Py-C2), 151.5 (Py-C6), 139.0 (Py-C4), 124.9 (Py-C3), 123.7 (Py-C5), 75.9 (d, J(Rh,C) = 13.8 Hz; −CH=CH−), 64.1 (N-CH_2-CH_2-CH_2-CH_3), 63.4 (N-CH_2-Py), 31.4 (C=C-CH_2), 27.2 (N-CH_2-CH_2-CH_2-CH_3), 21.0 (N-CH_2-CH_2-CH_2-CH_3), 14.0 (N-CH_2-CH_2-CH_2-CH_3); FAB-MS (NBA/CH_3CN): m/z: 466 $[M]^+$, 1077 $[2M+PF_6]^+$; $C_{24}H_{33}N_3RhPF_6$ (611.41): calcd C 47.15, H 5.44, N 6.87; found: C 46.43, H 5.33, N 6.84.

(η^4-Cycloocta-1,5-diene)-[κ^3-*fac*-*N*-benzyl-*N*,*N*-di(2-pyridylmethyl)amine]-rhodium(I)hexafluorophosphate ([5]PF_6): Compound [**5**]PF_6 was prepared by a procedure similar to described that for [**1**]PF_6, but with the ligand BzBPA. ^{1}H NMR (200.13 MHz, [D$_6$]acetone, 298 K): δ = 9.30 (d, ^3J(H,H) = 5.2 Hz, 2H; Py-H6), 7.90–7.10 (m, 11H; Py-H5, PyH4, Py-H3, *Ph*), 5.43 (s, 2H; N-CH_2-Ph), 4.98 (d[AB], ^2J(H,H) = 16.0 Hz, 2H; N-CH_2-Py), 4.03 (m, 4H; −CH=CH−), 3.86 (d[AB], ^2J(H,H) = 16.0 Hz, 2H; N-CH_2-Py), 2.76 (m, 4H; −C=C-CH_2-*exo*), 1.91 (m, 4H; −C=C-CH_2-*endo*); $^{13}C\{^1H\}$ NMR (50.33 MHz, [D$_6$]acetone, 298 K): δ = 159.8 (Py-C2), 151.8 (Py-C6), 138.9 (Py-C4), 134.3 (Ph-C1), 131.6 (Ph-C2), 129.1 (Ph-C3), 129.0 (Ph-C4), 124.8 (Py-C5), 123.9 (Py-C3), 76.2 (d, J(Rh,C) = 14.7 Hz; −CH=CH−), 67.3 (N-CH_2-Ph), 62.9 (N-CH_2-Py), 31.4 (C=C-CH_2); ^{1}H NMR indicates the presence of 0.5 mol H_2O per mol [(BzBPA)Rh(cod)]$^+$; FAB-MS (NBA/CH_3CN): m/z: 500 $[M]^+$, 1145 $[2M+PF_6]^+$. $C_{27}H_{32}O_{0.5}N_3RhPF_6$ (654.44): calcd C 49.55, H 4.93, N 6.42; found: C 49.31, H 4.50, N 6.41.

(η^4-Cycloocta-1,5-diene)-{κ^3-*fac*-*N*-butyl-*N*,*N*-di[(6-methyl-2-pyridyl)-methyl]amine}rhodium(I)hexafluorophosphate ([6]PF_6): Compound [**6**]PF_6 was prepared by a procedure similar to that described for [**1**]PF_6, but with the ligand BuBLA. ^{1}H NMR (200.13 MHz, [D$_6$]acetone, 298 K): δ = 7.75 (t, ^3J(H,H) = 7.6 Hz, 2H; Py-H4), 7.45 (d, ^3J(H,H) = 7.5 Hz, 2H; Py-H3), 7.32 (d, ^3J(H,H) = 7.6 Hz, 2H; Py-H5), 4.78 (d[AB], ^2J(H,H) = 16.0 Hz, 2H; N-CH_2-Py), 4.03 (d[AB], ^2J(H,H) = 16.0 Hz, 2H; N-CH_2-Py), 3.55 (s, 6H; Py-CH_3), 3.94 (m, 2H; N-CH_2-C_3H_7), 3.55 (s, 6H; Py-CH_3), 3.50 (m, 4H; −CH=CH−), 2.64 (m, 4H; −C=C-CH_2-*exo*), 1.92 (m, 2H; N-CH_2-CH_2-C_2H_5), 1.73 (m, 4H; −C=C-CH_2-*endo*), 1.53 (m, 2H; N-C_2H_4-CH_2-CH_3), 1.06 (t, ^3J(H,H) = 7.3 Hz, 3H; N-C_3H_6-CH_3); $^{13}C\{^1H\}$ NMR (75.47 MHz, [D$_6$]acetone, 298 K): δ = 162.2 (Py-C2), 161.4 (Py-C6), 139.6 (Py-C4), 126.9 (Py-C5), 122.3 (Py-C3), 76.5 (br s, −CH=CH−), 61.7 (N-CH_2-Py), 60.4 (N-CH_2-C_3H_7), 31.7 (C=C-CH_2), 29.7 (Py-CH_3), 26.1 (N-CH_2-CH_2-C_2H_5), 21.8 (N-C_2H_4-CH_2-CH_3), 14.7 (N-C_3H_6-CH_3); FAB-MS (NBA/CH_3CN): m/z: 494 $[M]^+$, 386 $[M-cod]^+$; $C_{26}H_{37}N_3RhPF_6$ (639.46): calcd C 48.84, H 5.83, N 6.57; found C 48.19, H 5.78, N 6.45.

(η^4-Cycloocta-1,5-diene)-{κ^3-*fac*-*N*-benzyl-*N*,*N*-di[(6-methyl-2-pyridyl)-methyl]amine}rhodium(I)hexafluorophosphate ([7]PF_6): Compound [**7**]PF_6 was prepared by a procedure similar to that described for [**1**]PF_6, but with the ligand BzBLA. ^{1}H NMR (200.13 MHz, [D$_6$]acetone, 298 K): δ = 7.75–7.45 (m, Ph-H2, Ph-H3, Ph-H4), 7.72 (t, ^3J(H,H) = 7.6 Hz, 2H; Py-H4), 7.42 (d, ^3J(H,H) = 7.5 Hz, 2H; Py-H3), 7.27 (d, ^3J(H,H) = 7.6 Hz, 2H; Py-H5), 5.06 (s, 2H; N-CH_2-Ph), 4.88 (d[AB], ^2J(H,H) = 15.8 Hz, 2H; N-CH_2-Py), 3.82 (d[AB], ^2J(H,H) = 15.8 Hz, 2H; N-CH_2-Py), 3.55 (s, 6H; Py-CH_3), 3.94 (m, 2H; N-CH_2-C_3H_7), 3.57 (m, 10H; −CH=CH−, Py-CH_3), 2.71 (m, 4H; −C=C-CH_2-*exo*), 1.75 (m, 4H; −C=C-CH_2-*endo*); $^{13}C\{^1H\}$ NMR (75.47 MHz, [D$_6$]acetone, 298 K): δ = 162.6 (Py-C2), 160.7 (Py-C6), 139.7 (Py-C4), 133.7 (Ph-C1), 133.3 (Ph-C2), 129.9 (Ph-C3), 129.8 (Ph-C4), 127.1 (Py-C5), 122.6 (Py-C3), 77.2 (br s, −CH=CH−), 62.7 (N-CH_2-Ph), 60.5 (N-CH_2-Py), 31.8 (C=C-CH_2), 29.8 (Py-CH_3); FAB-MS (NBA/CH_3CN): m/z: 528 $[M]^+$, 420 $[M-cod]^+$; $C_{29}H_{35}N_3RhPF_6$ (673.48): calcd C 51.72, H 5.24, N 6.34; found C 51.83, H 5.16, N 6.25.

Bis-(η^4-cycloocta-1,5-diene)-[μ-(bis-κ^3-*fac*)-*N*,*N*,*N*′,*N*′-tetrakis-(2-pyridylmethyl)-1,4-butanediamine]bis-rhodium(I)bis(hexafluorophosphate) ([8][PF_6]$_2$): The dinuclear complex $[8]^{2+}$ was prepared by the reaction of [{(cod)Rh(μ-Cl)}$_2$] with the ditopic ligand TPBN[35] in a 1:1 ratio, and isolated as [**8**][PF_6]$_2$ by a procedure similar to that described for [**1**]PF_6. ^{1}H NMR (400.14 MHz, CD_3CN, 298 K): δ = 9.16 (d, ^3J(H,H) = 5.1 Hz, 4H; Py-H6), 7.64 (m, 4H; Py-H4), 7.23 (m, 4H; Py-H5), 7.16 (d, ^3J(H,H) = 7.8 Hz, 4H; Py-H3), 4.48 (d[AB], ^2J(H,H) = 16.3 Hz, 4H; N-CH_2-Py), 4.12 (d[AB], ^2J(H,H) = 16.3 Hz, 4H; N-CH_2-Py), 4.08 (m, 4H; N-CH_2), 3.79 (m, 8H; −CH=CH−), 2.64 (m, 8H; −C=C-CH_2-*exo*), 2.24 (m, 4H; N-CH_2-CH_2−), 1.86 (m, 8H; −C=C-CH_2-*endo*); $^{13}C\{^1H\}$ NMR (100.614 MHz, CD_3CN, 298 K): δ = 160.5 (Py-C2), 152.0 (Py-C6), 139.4 (Py-C4), 125.3 (Py-C3), 124.1 (Py-C5), 76.6 (d, J(Rh,C) = 13.4 Hz; −CH=CH−), 64.3 (N-CH_2−), 63.8 (N-CH_2-Py), 31.9 (C=C-CH_2), 23.4 (N-CH_2-CH_2−); FAB-MS (NBA/CH_3CN): m/z: 1019 $[M-PF_6]^+$, 663 $[M-Rh-cod-2PF_6]^+$, 437 $[M/2]^{2+}$; $C_{44}H_{56}N_6Rh_2P_2F_{12}$ (1164.70): calcd C 45.38, H 4.85, N 7.22; found C 44.98, H 4.62, N 7.31.

(η^4-Cycloocta-1,5-diene)-(κ^2-2-pyridylmethylamine)rhodium(I)hexafluorophosphate ([9]PF_6): Compound [**9**]PF_6 was prepared by a procedure similar to that described for [**1**]PF_6, but with the ligand PA (yield 67%). An alternative preparation of [**9**]PF_6, and the characterisation of this complex has been reported previously.[43] In addition we now provide the ^{13}C NMR data for [**9**]PF_6. $^{13}C\{^1H\}$ NMR (75.47 MHz, [D$_6$]acetone, 298 K): δ = 165.8 (Py-C2), 148.5 (Py-C6), 140.6 (Py-C4), 124.6 (Py-C3), 122.7 (Py-C5), 82.6 (br, −CH=CH−), 51.2 (NH_2-CH_2-Py), 30.5 (C=C-CH_2).

(η^4-1,5-Hexadiene)-(κ^3-1,4,7-trimethyl-1,4,7-triazacyclononane)rhodium(I)-hexafluorophosphate ([10]PF_6): Cn* (100 mg, 0.58 mmol) and [{(hed)Rh(μ-Cl)}$_2$] (129 mg, 0.29 mmol) were stirred in MeOH (25 mL) for 1 hour. Subsequently, NH_4PF_6 (350 mg, 2.15 mmol) was added. Partial evaporation of the solvent caused the precipitation of [**10**]PF_6 as a yellow powder, which was filtered and vacuum dried. Yield 69% (200 mg); ^{1}H NMR (200.13 MHz, CD_3CN, 298 K): δ = 4.24 (m, 2H; −CH=CH_2), 3.0–2.65 (m, 12H; N-CH_2−), 2.78 (d, ^3J(Rh,H) = 0.6 Hz, 9H; N-CH_3), 2.41 (m, 2H; C=C-CH_2-*exo*), 2.02 (ddd, $^3J(H,H)_{cis}$ = 7.9 Hz, $^2J(H,H)_{gem}$ = 0.5 Hz, J(Rh,H) = 2.1 Hz, 2H; −CH=CH_cH$_t$), 1.76 (ddd, $^3J(H,H)_{trans}$ = 12.3 Hz, $^2J(H,H)_{gem}$ = 0.5 Hz, J(Rh,H) = 0.9 Hz, 2H; −CH=CH$_c$$H_t$), 1.55 (m, 2H; −C=C-$CH_2$-*endo*); $^{13}C\{^1H\}$ NMR (50.33 MHz, CD_3CN, 298 K): δ = 83.8 (d, J(Rh,C) = 12.8 Hz; −CH=CH_2), 58.1 (N-CH_2−), 50.5 (N-CH_3), 44.9 (d, J(Rh,C) = 14.4 Hz; −CH=CH_2), 33.6 (C=C-CH_2); FAB-MS (NBA/CH_3CN): m/z: 356 $[M-PF_6]^+$, 909 $[2M-PF_6]^+$; $C_{15}H_{31}N_3RhPF_6$ (501.296): calcd C 35.94, H 6.23, N 8.38; found: C 35.48, H 5.88, N 8.25.

(η^4-1,5-Hexadiene)-{κ^3-*fac*-*N*-benzyl-*N*,*N*-di[(6-methyl-2-pyridyl)methyl]-amine}rhodium(I)hexafluorophosphate ([11]PF_6): Compound [**11**]PF_6 was prepared by a procedure similar to that described for [**10**]PF_6, but with the ligand BzBLA. ^{1}H NMR (200.13 MHz, [D$_6$]acetone, 298 K): δ = 7.80–7.50 (m, Ph-H2, Ph-H3, Ph-H4), 7.73 (t, ^3J(H,H) = 7.6 Hz, 2H; Py-H4), 7.41 (d, ^3J(H,H) = 7.5 Hz, 2H; Py-H3), 7.31 (d, ^3J(H,H) = 7.6 Hz, 2H; Py-H5), 5.15 (br s, 2H; N-CH_2-Ph), 4.98 (d[AB], ^2J(H,H) = 15.8 Hz, 2H; N-CH_2-Py), 4.43 (m, 2H; −CH=CH_2), 3.78 (d[AB], ^2J(H,H) = 15.8 Hz, 2H; N-CH_2-Py), 3.51 (s, 6H; Py-CH_3), 2.77 (m, 2H; C=C-CH_2-*exo*), 2.48 (m, 2H; −CH=CH_cH$_t$), 2.20 (m, 2H; −CH=CH$_c$$H_t$), 1.83 (m, 2H; −C=C-$CH_2$-*endo*); $^{13}C\{^1H\}$-NMR (75.47 MHz, [D$_6$]acetone, 298 K): δ = 161.7 (Py-C2), 160.1 (Py-C6), 139.0 (Py-C4), 133.3 (Ph-C1), 133.5 (Ph-C2), 129.3 (Ph-C3), 129.2 (Ph-C4), 126.3 (Py-C5), 122.1 (Py-C3), 84.5 (br, −CH=CH_2), 64.0 (br, N-CH_2-Ph), 61.1 (N-CH_2-Py), 49.9 (d, J(C,Rh) = 13.9 Hz, −CH=CH_2), 34.4 (br, C=C-CH_2), 29.8 (Py-CH_3); FAB-MS (NBA/CH_3CN): m/z: 502 $[M]^+$, 420 $[M-(hed)]^+$; $C_{27}H_{33}N_3RhPF_6$ (647.44): calcd C 50.09, H 5.14, N 6.49; found C 49.92, H 5.01, N 6.49.

(9-Oxabicyclo[4.2.1]nona-2,5-diyl)-(κ^3-1,4,7-trimethyl-1,4,7-triazacyclononane)rhodium(III)hexafluorophosphate ([12]PF_6): Compound [**2**]PF_6 (37 mg) was dissolved in MeOH (5 mL) and 35% aqueous H_2O_2 solution (0.1 mL) was added. The solution was stirred at RT for 1 hour. Addition of Et_2O caused the precipitation of [**12**]PF_6 as a light yellow powder, which was filtered, washed with Et_2O, and vacuum dried. Yield 100% (38 mg). A similar reaction with [**2**]BPh_4 gave [**12**]BPh_4. ^{1}H NMR (200.13 MHz, [D$_6$]acetone, 298 K): δ = 5.95 (m, 2H; O-CH−), 3.35–3.15 (m, 4H; N-CH_2−), 3.18 (s, 6H; N-CH_3), 3.15–3.05 (m, 4H; N-CH_2−), 2.95–2.73 (m, 4H; N-CH_2−), 2.68 (m, 2H; Rh-CH−), 2.63 (d, ^3J(Rh,H) = 1.7 Hz, 3H; N-CH$_3$), 2.29–1.96 (m, 4H; Rh-CH-CH_2-*exo*/O-CH-CH_2-*exo*), 1.53 (m, 2H; O-CH-CH_2-*endo*), 1.41 (m, 2H; Rh-CH-CH_2-*endo*); $^{13}C\{^1H\}$ NMR (50.33 MHz, [D$_6$]acetone, 298 K): δ = 107.3 (d, ^2J(Rh,C) = 4.6 Hz; O-CH−), 62.3, 58.3 and 56.1 (N-CH_2−), 54.5 and 49.6 (N-CH_3), 28.1 and 27.0 (Rh-CH-CH_2−/O-CH-CH_2−), 21.7 (d, ^1J(Rh,C) = 23.0 Hz; Rh-CH−); FAB-MS (NBA/CH_3CN): m/z: 398 $[M]^+$, 941 $[2M+PF_6]^+$; $C_{17}H_{33}N_3ORhPF_6$ (543.33): calcd C 37.58, H 6.12, N 7.73; found C 37.26, H 5.93, N 7.65.

(9-Oxabicyclo[4.2.1]nona-2,5-diyl)-[κ^3-*fac*-*N*,*N*-di(2-pyridylmethyl)amine]-rhodium(III)tetraphenylborate ([13a]BPh_4): BPA (160 mg, 0.80 mmol) and [{(cod)Rh(μ-Cl)}$_2$] (192 mg, 0.39 mmol) were stirred in MeOH (25 mL) for 1 hour. The solution was cooled to −10 °C, and 35% aqueous H_2O_2 solution (0.2 mL) was added. Subsequently, $NaBPh_4$ (290 mg, 0.85 mmol) was added, resulting in the precipitation of [**13a**]BPh_4 as a white/light

yellow powder, which was filtered and vacuum dried. Yield 77% (459 mg); ^{1}H NMR (200.130 MHz, CD_2Cl_2, 298 K): $\delta = 8.86$ (d, $^3J(H,H) = 5.0$ Hz, 1H; Py-H6), 8.11 (d, $^3J(H,H) = 5.0$ Hz, 1H; Py-H6), 7.44 (m, 8H; BAr-H2), 7.80–6.75 (m, 6H; Py-H4, Py-H5, Py-H3), 7.06 (t,$^3J(H,H) = 7.4$ Hz, 8H; BAr-H3), 6.84 (t, $^3J(H,H) = 7.4$ Hz, 4H; BAr-H4), 5.98 (m, 1H; O-CH−), 5.83 (m, 1H; O-CH−), 4.24 (dd[AB], $^2J(H,H) = 17.4$ Hz, $^3J(NH,H) = 7.4$ Hz, 1H; N-CH_2-Py), 3.93 (dd[AB], $^2J(H,H) = 16.7$ Hz, $^3J(NH,H) = 6.8$ Hz, 1H; N-CH_2-Py), 3.75 (m, 1H; NH), 3.48 (dd[AB], $^2J(H,H) = 17.4$ Hz, $^3J(NH,H) = 1.3$ Hz, 1H; N-CH_2-Py), 3.29 (d[AB], $^2J(H,H) = 16.7$ Hz, 1H; N-CH_2-Py), 3.02 (m, 1H; Rh-CH−), 2.98 (m, 1H; Rh-CH−), 2.3–2.0 (m, 4H; Rh-CH-CH_2-*exo*/O-CH-CH_2-*exo*), 1.85–1.4 (m, 4H; O-CH-CH_2-*endo*/Rh-CH-CH_2-*endo*), 1.45 (s, ≈2H; H_2O); ^{13}C{^{1}H} NMR (50.33 MHz, CD_2Cl_2, 298 K): $\delta = 164.9$ (q, $^1J(C,B) = 49.0$ Hz; BAr-C1), 162.3 (Py_a-C2), 161.0 (Py_b-C2), 152.6 (Py_a-C6), 150.0 (Py_b-C6), 138.4 (Py_a-C4), 137.0 (Py_b-C4), 136.9 (BAr-C2), 126.5 (q, $^3J(C,B) = 2.8$ Hz; BAr-C3), 124.8 (Py_a-C3), 124.6 (Py_b-C3), 123.1 (Py_a-C5), 122.7 (BAr-C4),122.6 (Py_b-C5), 107.9 (O-CH_a−), 106.8 (O-CH_b−), 59.9 (N-CH_2-Py_a), 59.0 (N-CH_2-Py_b), 29.6, 29.2, 27.4 and 26.6 (Rh-CH-CH_2−/O-CH-CH_2−), 25.6 (d, $^1J(Rh,C) = 20.8$ Hz; Rh-CH_a−), 20.8 (d, $^1J(Rh,C) = 19.4$ Hz; Rh-CH_b); FAB-MS (NBA/CH_3CN): *m/z*: 426 $[M]^+$; $C_{44}H_{45}N_3ORhB \cdot H_2O$ (763.59): calcd C 69.21, H 6.20, N 5.50; found C 69.18, H 5.66, N 5.58.

(9-Oxabicyclo[4.2.1]nona-2,5-diyl)-[κ^3-*fac*-*N*-butyl-*N*,*N*-di(2-pyridylmethyl)amine]rhodium(III)hexafluorophosphate ([14a]PF_6): Compound [**14a**]PF_6 was prepared by a method similar to that described for [**12**]PF_6, except that the reaction was carried out at −10 °C. ^{1}H NMR (200.13 MHz, [D$_6$]acetone, 298 K): $\delta = 9.23$ (d, $^3J(H,H) = 5.4$ Hz, 1H; Py-H6), 8.50 (d, $^3J(H,H) = 5.6$ Hz, 1H; Py-H6), 7.10–8.10 (m, 6H; Py-H4, Py-H5, Py-H3), 6.08 (m, 1H; O-CH−), 6.04 (m, 1H; O-CH−), 4.85 (d[AB], $^2J(H,H) = 15.6$ Hz, 1H; N-CH_2-Py), 4.67 (d[AB], $^2J(H,H) = 17.2$ Hz, 1H; N-CH_2-Py), 4.53 (d[AB], $^2J(H,H) = 15.6$ Hz, 1H; N-CH_2-Py), 4.16 (d[AB], $^2J(H,H) = 17.2$ Hz, 1H; N-CH_2-Py), 3.90–3,45 (m, 2H; N-CH_2-CH_2-CH_2-CH_3), 3.42 (m, 1H; Rh-CH−), 2.91 (m, 1H; Rh-CH−), 2.3–2.0 (m, 4H; Rh-CH-CH_2-*exo*/O-CH-CH_2-*exo*), 1.85–1.05 (m, 8H; O-CH-CH_2-*endo*/Rh-CH-CH_2-*endo*/N-CH_2-CH_2-CH_2-CH_3/N-CH_2-CH_2-CH_2-CH_3), 0.91 (t, $^3J(H,H) = 7.4$ Hz, 3H; N-CH_2-CH_2-CH_2-CH_3); ^{13}C{^{1}H} NMR (50.33 MHz, [D$_6$]acetone, 298 K): $\delta = 162.5$ (Py_a-C2), 161.5 (Py_b-C2), 153.8 (Py_a-C6), 150.8 (Py_b-C6), 139.0 (Py_a-C4), 137.6 (Py_b-C4), 125.2 (Py_a-C3), 125.0 (Py_b-C3), 123.6 (Py_a-C5), 122.2 (Py_b-C5), 106.6 (d, $^2J(Rh,C) = 4.0$ Hz; O-CH_a−), 105.7 (d, $^2J(Rh,C) = 4.0$ Hz; O-CH_b−), 66.4 (N-CH_2-CH_2-CH_2-CH_3), 63.3 (N-CH_2-Py_a), 63.2 (N-CH_2-Py_b), 28.8 (N-CH_2-CH_2-CH_2-CH_3), 28.2, 27.7, 26.7 and 26.6 (Rh-CH-CH_2−/O-CH-CH_2−), 25.2 (d, $^1J(Rh,C) = 19.4$ Hz; Rh-CH_a−), 23.5 (d, $^1J(Rh,C) = 19.4$ Hz; Rh-CH_b−), 20.9 (N-CH_2-CH_2-CH_2-CH_3), 13.9 (N-CH_2-CH_2-CH_2-CH_3); FAB-MS (NBA/CH_3CN): *m/z*: 482 $[M]^+$; $C_{24}H_{33}N_3ORhPF_6$ (627.41): calcd C 45.95, H 5.36, N 6.76; found C 44.29, H 5.07, N 6.45.

[1,4,5,6-η^4-(2-Hydroxycycloocta-4-ene-1,6-di-yl)]-(κ^3-1,4,7-trimethyl-1,4,7-triazacyclononane)rhodium(III)hexafluorophosphate/tetraphenylborate ([15]PF_6/BPh_4): Compound [**15**]PF_6 was obtained by heating [**12**]PF_6 to 80 °C for 12 hours in CH_3CN, followed by evaporation of the solvent under reduced pressure, yield 100%. Similarly, [**15**]BPh_4 was prepared by heating [**12**]BPh_4. Assignment of NMR signals of the Rh^{III}(cycloocta-2-hydroxy-4,5-ene-1,6-di-yl) fragment is in accordance with the atom labelling in Figure 9. ^{1}H-NMR (400.136 MHz, [D$_6$]DMSO, 298 K): $\delta = 7.31$ (m, 8H; BAr-H2), 7.03 (t,$^3J(H,H) = 7.3$ Hz, 8H; BAr-H3), 6.87 (t, $^3J(H,H) = 7.3$ Hz, 4H; BAr-H4), 4.64 (s, 1H; OH), 4.47 (m, 1H; allyl-H21), 4.22 (m, 1H; allyl-H23), 4.04 (t, $^3J(H,H) = 8.5$ Hz, 1H; allyl-H22), 3.45 (s, 3H; N-CH_3), 3.35–2.2 (m, 12H; N-CH_2−), 3.10 (s, 3H; N-CH_3), 3.06 (m, 1H; C*H*(OH) (H12)), 2.43–2.35 (m, 2H; Rh-C*H* (H11), Rh-CH-CH_2-*exo* (H14B)), 2.24 (s, 3H; N-CH_3), 2.08 (m, 1H; allyl-CH_2-*exo* (H13B)), 1.80 (m, 1H; allyl-CH_2-*exo* (H24B)), 1.74 (m, 1H; allyl-CH_2-*endo* (H13A)), 0.90 (m, 1H; Rh-CH-CH_2-*endo* (H14A)).0.71 (m, 1H; allyl-CH_2-*endo* (H24A)); ^{13}C{^{1}H} NMR (100.614 MHz, [D$_6$]acetone, 298 K): $\delta = 163.3$ (q, $^1J(C,B) = 49.2$ Hz; BAr-C1), 135.5 (BAr-C2), 125.3 (q, $^3J(C,B) = 2.8$ Hz; BAr-C3), 121.5 (BAr-C4), 94.9 (d, $^1J(Rh,C) = 5.8$ Hz; allyl-C22), 84.0 (*C*HOH (C12)), 70.6 (d, $^1J(Rh,C) = 12.2$ Hz; allyl-C21), 63.9 (N-CH_2−), 63.3 (d, $^1J(Rh,C) = 12.7$ Hz; allyl-C23), 61.2 (N-CH_2−), 58.5 (N-CH_2−), 58.0 (N-CH_2−), 57.1 (d, $^1J(Rh,C) = 24.8$ Hz; Rh-*C*H− (C11)), 56.3 (N-CH_3), 56.0 (N-CH_2−), 55.0 (N-CH_3), 53.4 (N-CH_2−), 49.2 (N-CH_3), 41.0 (RhCH-CH_2− (C14)), 37.3 (allyl-CH_2− (C13)), 23.7 (allyl-CH_2− (C24)); FAB-MS (NBA/CH_3CN): *m/z*: 398 $[M - PF_6]^+$, 941 $[2M - PF_6]^+$; [**15**]BPh_4 $C_{41}H_{53}N_3ORhB$ (717.61): calcd C 68.62, H 7.44, N 5.86; found C 68.07, H 7.49, N 5.91; [**15**]PF_6 $C_{17}H_{33}N_3ORhPF_6$ (543.33): calcd C 37.58, H 6.12, N 7.73; found C 37.23, H 6.05, N 7.68.

[1,4,5,6-η^4-(2-Hydroxycycloocta-4-ene-1,6-di-yl)]-[κ^3-*fac*-*N*,*N*-di(2-pyridylmethyl)amine]rhodium(III)tetraphenylborate ([16a]BPh_4): Compound [**16a**]BPh_4 was obtained by heating [**13a**]BPh_4 to 40 °C for 5 hours in CH_2Cl_2, followed by evaporation of the solvent under reduced pressure, yield 100%. Assignment of NMR signals of the Rh^{III}(cycloocta-2-hydroxy-4,5-ene-1,6-di-yl) fragment is in accordance with the atom labelling in Figure 8. ^{1}H NMR (400.136 MHz, [D$_6$]acetone, 298 K): $\delta = 9.34$ (d, $^3J(H,H) = 5.4$ Hz, 1H; Py-H6), 8.21 (d, $^3J(H,H) = 5.2$ Hz, 1H; Py-H6), 8.00 (m, 1H; NH), 7.77 (m, 1H; Py-H4), 7.66 (m, 1H; Py-H4), 7.36 (m, 8H; BAr-H2), 7.40–7.30 (m, 3H; Py-H5 and Py-H3), 7.18 (m, 1H; Py-H5), 7.01 (t, $^3J(H,H) = 7.4$ Hz, 8H; BAr-H3), 6.86 (t, $^3J(H,H) = 7.4$ Hz, 4H; BAr-H4), 5.14 (m, 1H; allyl-H21), 5.00 (dd[AB], $^2J(H,H) = 18.05$ Hz, $^3J(NH,H) = 8.42$ Hz, 1H; N-CH_2-Py), 4.90 (dd[AB], $^2J(H,H) = 16.38$ Hz, $^3J(NH,H) = 6.45$ Hz, 1H; N-CH_2-Py), 4.62 (s, 1H; OH), 4.61 (m, 1H; allyl-H23), 4.42 (dd[AB], $^2J(H,H) = 16.38$ Hz, $^3J(NH,H) = 1.02$ Hz, 1H; N-CH_2-Py), 4.37 (ddd, $^3J(H,H) = 8.5$ Hz, $^3J(H,H) = 7.72$ Hz, $^2J(Rh,H) = 1.6$ Hz, 1H; allyl-H22), 4.32 (d[AB], $^2J(H,H) = 18.05$ Hz, 1H; N-CH_2-Py), 3.60 (m, 1H; C*H*(OH) (H12)), 2.33 (m, 1H; Rh-C*H* (H11)), 2.14 (m, 1H; allyl-CH_2-*exo* (H24B)), 2.07 (m, 1H; allyl-CH_2-*exo* (H13B)), 1.97 (m, 1H; Rh-CH-CH_2-*exo* (H14B)), 1.54 (m, 1H; allyl-CH_2-*endo* (H13A)), 1.42 (m, 1H; allyl-CH_2-*endo* (H24A)), 1.15 (m, 1H; Rh-CH-CH_2-*endo* (H14A)); ^{13}C{^{1}H} NMR (100.614 MHz, [D$_6$]acetone, 298 K): $\delta = 165.1$ (q, $^1J(C,B) = 48.6$ Hz; BAr-C1), 162.7 (Py_a-C2), 160.0 (Py_b-C2), 154.8 (Py_a-C6), 149.9 (Py_b-C6), 139.6 (Py_a-C4), 137.7 (BAr-C2), Py_b-C4 obscured by BAr-C2 signal, 126.0 (Py_a-C3), 126.7 (q, $^3J(C,B) = 2.8$ Hz; BAr-C3), 125.9 (Py_b-C3), 123.8 (Py_a-C5), 123.7 (Py_b-C5), 122.9 (BAr-C4), 99.0 (d, $^1J(Rh,C) = 5.3$ Hz; allyl-C22), 88.5 (*C*HOH (C12)), 74.4 (d, $^1J(Rh,C) = 12.4$ Hz; allyl-C21), 66.7 (d, $^1J(Rh,C) = 12.2$ Hz; allyl-C23), 64.1 (N-CH_2-Py), 61.0 (N-CH_2-Py), 52.0 (d, $^1J(Rh,C) = 21.1$ Hz; Rh-*C*H- (C11)), 39.8 (RhCH-CH_2− (C14)), 36.8 (allyl-CH_2− (C13)), 25.2 (allyl-CH_2− (C24)); FAB-MS (NBA/CH_3CN): $C_{20}H_{25}N_3ORh$: calcd 426.1053; found 426.1062 $[M - BPh_4]^+$; $C_{44}H_{45}N_3ORhB$ (745.58): calcd C 70.88, H 6.08, N 5.64; found C 70.92, H 5.61, N 5.82.

[1,4,5,6-η^4-(2-Hydroxycycloocta-4-ene-1,6-di-yl)]-[κ^3-*fac*-*N*-butyl-*N*,*N*-di-(2-pyridylmethyl)amine]rhodium(III)hexafluorophosphate ([17a]PF_6): Compound [**17a**]PF_6 was obtained by heating [**14a**]PF_6 to 80 °C for 12 hours in CH_2Cl_2, followed by evaporation of the solvent under reduced pressure. Yield 100%; ^{1}H NMR (200.13 MHz, [D$_6$]acetone, 298 K): $\delta =$ 9.40 (d, 1H; $^3J(H,H) = 5.3$ Hz; Py-H6), 8.20 (d, 1H; $^3J(H,H) = 5.5$ Hz; Py-H6), 8.00–7.00 (m, 6H; Py-H3, Py-H4, Py-H5), 5.20–4.50 (m, 8H; N-CH_2-Py, allyl-H21, -H22, -H23, OH), 4.20–3.80 (m, 2H; N-CH_2-C_3H_7), 3.50 (m, 1H; C*H*(OH) (H12)), 2.80–0.7 (m, 14H; Rh-C*H*, allyl-CH_2-*exo*, allyl-CH_2-*endo*, −CH_2−CH_2-CH_3); ^{13}C{^{1}H} NMR (75.48 MHz, [D$_6$]acetone, 298 K): $\delta = 159.7$ (Py_a-C2), 158.0 (Py_b-C2), 155.7 (Py_a-C6), 148.3 (Py_b-C6), 138.8 (Py_a-C4), 138.5 (Py_b-C4), 125.0 (Py_a-C3), 123.5 (Py_b-C3), 122.7 (Py_a-C5), 122.2 (Py_b-C5), 98.3 (d, $^1J(Rh,C) = 5.3$ Hz; allyl-C22), 89.0 (*C*HOH (C12)), 71.2 (d, $^1J(Rh,C) = 11.6$ Hz; allyl-C21), 70.4 (d, $^1J(Rh,C) = 12.6$ Hz; allyl-C23), 68.4 (N-CH_2-Py), 68.1 (N-CH_2-Py), 67.1 (N-CH_2-C_3H_7), 53.2 (d, $^1J(Rh,C) = 22.1$ Hz; Rh-*C*H− (C11)), 38.1 (RhCH-CH_2− (C14)), 34.1 (allyl-CH_2− (C13)), 26.6 (N-CH_2-CH_2-C_2H_5), 25.6 (allyl-CH_2− (C24)), 20.9 (N-C_2H_4-CH_2-CH_3), 14.0 (N-C_3H_6-CH_3).

(η^4-Cycloocta-1,5-diene)-(κ^2-(*N*-(2-pyridiniumylmethyl)-2-pyridylmethanamine]rhodium(I)hexafluorophosphate-tetra[3,5-di(trifluoromethyl)phenyl]borate ([18][PF_6][BAr^f_4]): Compound [**18**][PF_6][BAr^f_4] was prepared by addition of $HBAr^f_4$[23] (91 mg, 0.09 mmol) to a solution of [**3**]PF_6 (50 mg, 0.09 mmol) in CH_2Cl_2 (10 mL), followed by evaporation of the solvent. ^{1}H NMR (400.14 MHz, CD_2Cl_2, 225 K): $\delta = 15.9$ (br s, Py*H*), 8.49 (dd, $^3J(H,H) = 7.8$ Hz, $^3J(H,H) = 7.6$ Hz, PyH-*H6*), 8.60–7.25 (19H; Py, PyH, B(Ar^f)$_4$), 4.72 (br m, NH), 4.51 (m, 1H; *HC*=CH), 4.37 (m, 1H; *HC*=CH), 4.27 (d[AB], $^3J(H,H) = 16.6$ Hz, N-CH_2-Py), 4.19 (m, 1H; *HC*=CH), 4.12 (d[AB], $^3J(H,H) = 14.0$ Hz, N-CH_2-PyH), 4.01 (m, 1H; *HC*=CH), 3.96 (d[AB], $^3J(H,H) = 14.0$ Hz, N-CH_2-PyH), 3.80 (d[AB], $^3J(H,H) = 16.6$ Hz, N-CH_2-Py), 2.50–1.75 (8H; C=C-CH_2−); ^{13}C{^{1}H} NMR (100.61 MHz, CD_2Cl_2, 225 K): $\delta = 157.9$, 147.9, 147.5, 147.3, 142.7, 140.6, 129.1, 127.7, 125.1 and 122.9 (Py and PyH), 85.3, 84.6, 83.9 and 82.6 (br, *CH*=CH), 55.5 and 50.5 (N-CH_2-Py_b), 30.7, 29.7, 29.5 and 28.7 (C=C-CH_2).

0947-6539/99/0510-2934 $ 17.50+.50/0 *Chem. Eur. J.* **1999**, *5*, No. 10

Acknowlegments

We thank Unilever Research Laboratory, Vlaardingen, for a generous gift of 1,4,7-trimethyl-1,4,7-triazacyclononane. We thank Johnson Matthey for a generous loan of $RhCl_3 \cdot 3H_2O$.

[1] a) T. G. Spiro, *Metal Ion Activation of Dioxygen*, **1980**, Wiley; b) R. S. Drago, *Coord. Chem. Rev.* **1992**, *117*, 185; c) D. H. R. Barton, *The Activation of Dioxygen and Homogeneous Catalytic Oxidation*, **1993**, Plenum, New York; d) R. S. Drago, R. H. Beer, *Inorg. Chim. Act.* **1992**, *198–200*, 359; e) H. Mimoun, *Compr. Coord. Chem.* **1987**, *6*, 317; f) R. H. Holm, *Chem. Rev.* **1987**, 87, 1401; g) R. A. Sheldon, J. K. Kochi, *Metal-Catalyzed Oxidations of Organic Compounds*, **1981**, Academic, New York.

[2] Examples of the use of O_2 in bulk olefin oxidation: Wacker process (ethene to acetaldehyde), SMPO process (propene to propeneoxide and ethylbenzene to styrene), EO process (ethene to etheneoxide).

[3] See: p. 72 in ref. [1c] and chapter 3 in ref. [1g].

[4] See for example: a) C. Dudley, G. Read, *Tetrahedron Lett.* **1972**, *52*, 5273; b) E. D. Nyberg, D. C. Pribich, R. S. Drago, *J. Am. Chem. Soc.* **1983**, *105*, 3538; c) R. S. Drago, A. Zuzich, E. D. Nyberg, *J. Am. Chem. Soc.* **1985**, *107*, 2898; d) H. Minoun, M. Mercedes, P. Machirant, I. Sérée de Roch, *J. Am. Chem. Soc.* **1978**, *100*, 5437; e) see ref. [1g] f) R. S. Dickson, *Homogeneous Catalysis with Compounds of Rhodium and Iridium*, D Reidel Publishing Company, Dordrecht Holland, **1985**.

[5] P. Müller, H. Idmoumaz, *J. Organomet. Chem.* **1988**, *345*, 187.

[6] a) A. Fusi, R. Ugo, A. Pasini, S. Cenini, *J Organomet. Chem.* **1971**, *26*, 417; b) K. Kaneda, T. Itoh, Y. Fujiwara, S. Teranishi, *Bull. Chem. Soc. Jpn.* **1973**, *46*, 3810; c) A. Morvillo, M. Bressan, *J. Mol. Catal.* **1986**, *37*, 63; d) J. P. Collman, M. Kubota, J. W. Hosking, *J. Am. Chem. Soc.* **1967**, *89*, 4809; e) K. Takao, Y. Fujiwara, T. Imanaka, S. Teranishi, *Bull. Chem. Soc. Jpn.* **1970**, *43*, 1153.

[7] V. W. Day, W. G. Klemperer, S. P. Lockledge, D. J. Main, *J. Am. Chem. Soc.* **1990**, *112*, 2031.

[8] F. A. Cotton, P. Lahuerta, M. Sanau, W. Schwotzer, *Inorg. Chim. Act.* **1986**, *120*, 153.

[9] M. T. Atlay, M. Preece, G. Strukul, B. R. James, *J. Chem. Soc. Chem. Commun.* **1982**, 406.

[10] B. de Bruin, M. J. Boerakker, J. J. J. M. Donners, B. E. C. Christiaans, P. P. J. Schlebos, R. de Gelder, J. M. M. Smits, A. L. Spek, A. W. Gal, *Angew. Chem.* **1997**, *109*, 2153; *Angew. Chem. Int. Ed. Engl.* **1997**, *36*, 2064.

[11] A. R. Rossi, R. Hoffmann, *Inorg. Chem.* **1975**, *14*, 365.

[12] a) M. A. Esteruelas, F. J. Lahoz, A. M. Lopez, E. Onate, L. A. Oro, N. Ruiz, E. Sola, J. I. Tolosa, *Inorg. Chem.* **1996**, *35*, 7811; b) P. G. Rasmussen, O. H. Bailey, J. C. Bayon, *Inorg. Chem.* **1984**, *23*, 343; c) S. W. Kaiser, R. B. Saillant, W. M. Butler, P. G. Butler, P. G. Rasmussen, *Inorg. Chem.* **1976**, *15*, 2681; d) M. Akita, K. Ohta, Y. Takahashi, S. Hikichi, Y. Moro-Oka, *Organometallics* **1997**, *16*, 4121; e) M. Bortolin, U. E. Bucher, H. Rüegger, L. M. Venanzi, A. Albinati, F. Lianza, S. Trofimenko, *Organometallics* **1992**, *11*, 2514; f) H. Brunner, P. Beier, G. Riepl, I. Bernal, G. M. Reisner, R. Benn, A. Rufinska, *Organometallics* **1985**, *4*, 1732; g) K. A. Beveridge, G. W. Bushnell, S. R. Stobart, J. L. Atwood, M. J. Zaworotko, *Organometallics* **1983**, *2*, 1447; h) M. Cocivera, G. Ferguson, B. Kaitner, F. J. Lalor, D. J. O'Sullivan, M. Pavez, B. Ruhl, *Organometallics* **1982**, *1*, 1132; i) M. A. Garalda, R. Hernandez, L. Ibarlucea, M. I. Arriotua, M. K. Urtiaga, *Inorg. Chim. Acta* **1995**, *232*, 9; j) H. Brunner, G. Riepl, I. Bernal, W. H. Ries, *Inorg. Chim. Acta* **1986**, *112*, 65; k) M. P. Garcia, A. M. Lopez, M. A. Esteruelas, F. J. Lahoz, L. A. Oro, *J. Chem. Soc. Chem. Commun.* **1988**, 793; l) K. Yamamoto, H. Tateishi, W. Watanabe, T. Adachi, H. Matsubara, T. Ueda, T. Yoshida, *J. Chem. Soc. Chem. Commun.* **1995**, 1637; m) F. J. Lahoz, A. Tiripicchio, M. Tiripicchio Camellini, L. A. Oro, M. T. Pinillos, *J. Chem. Soc. Dalton Trans.* **1985**, 1487; n) D. Sanz, M. D. Santa Maria, R. M. Claramunt, M. Cano, J. V. Heras, J. A. Campo, F. A. Ruiz, E. Pinilla, A. Monge, *J. Organomet. Chem.* **1996**, *523*, 179; o) H. Brunner, B. Nubber, M. Prommesberger, *J. Organomet. Chem.* **1996**, *526*, 341; p) W. S. Sheldrick, B. Gunther, *J. Organomet. Chem.* **1991**, *402*, 256; q) W. S. Sheldrick, B. Gunther, *J. Organomet. Chem.* **1989**, *375*, 233; r) A. Albinati, C. Arz, P. S. Preggosin, *J. Organomet. Chem.* **1988**, *356*, 367; s) M. A. Esteruelas, L. A. Oro, M. C. Apreda, C. Foces-Foces, F. H. Cano, R. M. Claramunt, C. Lopez, J. Elguero, M. Begtrup, *J. Organomet. Chem.* **1988**, *344*, 93; t) L. A. Oro, M Esteban, R. M. Claramunt, J. Elguero, C. Foces-Foces, F. H. Cano, *J. Organomet. Chem.* **1984**, 276, 79; u) B.M Louie, S. J. Rettig, A. Storr, J. Trotter, *Can. J. Chem.* **1984**, *62*, 1057. v) W. H. Watson, A. Nagl, A. P. Marchand, P. Annapurna, *Acta Crystallogr. Sect. C* **1989**, *45*, 856.

[13] a) H. M. Colquhoun, S. M. Doughty, J. F. Stoddart, D. J. Williams, *J. Chem. Soc. Dalton Trans.* **1986**, 1639; b) A. A. H. van der Zeijden, G. Van Koten, R. A. Nordemann, B. Kojic-Prodic, A. L. Spek, *Organometallics* **1988**, *7*, 1957.

[14] a) U. E. Bucher, T. F. Fässler, M. Hunziker, R. Nesper, H. Rüegger, L. M. Venanzi, *Gazz. Chim. Ital.* **1995**, *125*, 181; b) M. Akita, K. Ohta, Y. Takahashi, S. Hikichi, Y. Moro-oka, *Organometallics* **1997**, *16*, 4121; c) U. E. Bucher, A. Currao, R. Nesper, H. Rüegger, L. M. Venanzi, E. Younger, *Inorg. Chem.* **1995**, *34*, 66; d) M. A. Esteruelas, L. A. Oro, M. C. Apreda, C. Foces-Foces, F. H. Cano, R. M. Claramunt, C. Lopez, J. Elguero, M. Begtrup, *J. Organomet. Chem.* **1988**, *344*, 93; e) M. C. López Gallego-Preciado, P. Ballesteros, R. M. Claramunt, M. Cano, J. V. Heras, E. Pinilla, A. Monge, *J. Organomet. Chem.* **1993**, *450*, 237.

[15] D. E. Axelson, C. E. Holloway, A. J. Oliver, *Inorg. Nucl. Chem. Lett.* **1973**, *9*, 885.

[16] The linear relation between E^{p}_{anode} and $\delta(^{13}C_{C=C})$ includes [{Rh^{I}(-cod)(μ_2-Cl)}$_2$]. Irreversible oxidation of the free ligands occurs at much higher potentials (e.g., BPA: $E^{p}_{anode} = 1080$ mV). Therefore, oxidation of the nitrogen-donor ligand can be excluded. In case of cod-centred oxidation, one would expect a much smaller influence of the nitrogen-donor ligand on the observed oxidation potential.

[17] U. E. Bucher, A. Currao, R. Nesper, H Rüeger, L. M. Venanzi, E. Younger, *Inorg. Chem.* **1995**, *34*, 66.

[18] a) H. C. Brown, *J. Am. Chem. Soc.* **1945**, *67*, 378, 1452; b) J. March, *Advanced Organic Chemistry*, 4th ed., Wiley, **1992**, p. 267, 270; c) H. C. Brown, H. Bartholomay, Jr., M. D. Taylor, *J. Am. Chem. Soc.* **1944**, *66*, 435.

[19] D. R. Russell, P. A. Tucker, *J. Chem. Soc. Dalton. Trans.* **1976**, 841.

[20] a) M. Alvarez, N. Lugan, R. Mathieu, *J. Organomet. Chem.* **1994**, *468*, 249; b) R. Graziani, G. Bombieri, L. Volponi, C. Panattoni, R. J. H. Clark, *J. Chem. Soc. A* **1969**, 1236; c) S. C. Haefner, K. R. Dunbar, C. Bender, *J. Am. Chem. Soc.* **1991**, *113*, 9540; d) G. E. Efe, E. O. Schlemper, *Polyhedron* **1991**, *10*, 1611; e) E. Lindner, Q. Wang, H. A. Meyer, R. Fawzi, M. Steimann, *J. Organomet. Chem.* **1993**, *453*, 289; f) S. J. Chadwell, S. J. Coles, P. G. Edwards, M. B. Hursthouse, *J. Chem. Soc. Dalton Trans.* **1995**, 3551.

[21] a) D. M. Walba, M. D. Wand, M. C. Wilkes, *J. Am. Chem. Soc.* **1979**, *101*, 4396; b) J. E. Baldwin, M. J. Crossley, E. M. M. Lehtonen, *J. Chem. Soc. Chem. Commun.* **1979**, 918.

[22] Most of the ^{1}H NMR signals of [**13a**]$^+$ are obscured by those of [**13b**]$^+$, yet some characteristic signals indicate its formation: ^{1}H NMR (200.13 MHz, [D$_6$]acetone, 298 K): $\delta = 8.95$ (d, ^3J(H,H) = 5.4 Hz, 2H; Py-H6), 5.92 (m, 2H; O-CH–), 2.77 (m, 2H; Rh-CH–).

[23] M. Brookhart, B. Grant, A. F. Volpe, Jr., *Organometallics* **1992**, *11*, 3920.

[24] a) P. Schuster, G. Zundel, C. Sandorfy, *The Hydrogen Bond*, North Holland, Amsterdam, **1976**; b) G. C. Pimentel, A. L. McClellan, *The Hydrogen Bond*, San Francisco, **1960**.

[25] ^{1}H NMR (200.13 MHz, [D$_6$]acetone, 298 K): $\delta = 9.55$ (d, ^3J(H,H) = 5.3 Hz, 1H; py-H6), 8.13–7.50 (br m, py-H3, Py-H4, Py-H5, NH), 6.46 (br m, 1H; NH), 5.00 (m, 1H; allyl-H21), 4.76 (m, 1H; allyl-H23), 4.65–4.40 (m, 3H; N-CH$_2$-Py, OH?), 4.23 (m, 1H; allyl-H23), 3.25 (m, 1H; C*H*(OH) (H12)), 2.6–0.5 (m, 7H; Rh-C*H*, allyl-CH$_2$-*exo*, allyl-CH$_2$-*endo*).

[26] H. Nishida, N. Takada, M. Yoshimura, T. Sonoda, H. Kobayashi, *Bull. Chem. Soc. Jpn.* **1984**, *57*, 2600, and references therein.

[27] P. W. Atkins, Physical Chemistry, 3rd ed., Oxord University Press, **1988**, pp. 693–694.

[28] The spectra of [**18**]$^{2+}$ clearly show the presence of two inequivalent pyridine groups and rhodium(I) coordinated cod. One of the Py-H6 signals is shifted upfield owing to the anisotropic-shielding effect of the olefin fragment like in [**9**]$^+$, whereas the PyH-H6 signal is

observed as a triplet. A signal at $\delta = 15.9$ is assigned to the pyridinium proton. Unlike for five-coordinate $[\mathbf{3}]^+$, rotation of the cod fragment is slow on NMR timescale at $-48\,^\circ C$ for $[\mathbf{18}]^+$.

[29] a) T. Kojima, R. A. Leising, S. Yan, L. Que, Jr., *J. Am. Chem. Soc.* **1993**, *115*, 11328; b) E. T. Denisov, I. V. Khudyakov, *Chem. Rev.* **1987**, *87*, 1313.

[30] a) J. E. Bäckvall, B. Åkermark, S. O. Ljunggren, *J. Am. Chem. Soc.* **1979**, *101*, 2411; b) J. K. Stille, R. Divakarani, *J. Organomet. Chem.* **1979**, *169*, 239.

[31] Oxidation of tertiary amines by H_2O_2 is thought to involve attack by the OH^+ moiety of H_2O_2: J. March, *Advanced Organic Chemistry*, 4th ed., Wiley, **1992**, p. 1200.

[32] I. I. Moiseev, *J. Mol. Catal. A* **1997**, *127*, 1.

[33] a) N. Wei, D-H. Lee, N. Murthy, Z Tyeklár, K. D. Karlin, S. Kaderli, B. Jung, A. D. Zuberbüler, *Inorg. Chem.* **1994**, *33*, 4625; b) K. D. Karlin, M. S. Haka, R. W. Cruse, G. J. Meyer, A. Farooq, Y. Gultneh, J. C. Hayes, J. Zubieta, *J. Am. Chem. Soc.* **1988**, *110*, 1196.

[34] Reaction of $[(\eta^5\text{-}C_5Me_5)(pz)Ir^{III}(\mu\text{-}pz)_2Rh^{I}(dppe)]$ with $HBF_4 \cdot OEt_2$ in the presence of air yields the hydroperoxo complex $[(\eta^5\text{-}C_5Me_5)\text{-}Ir^{III}(\mu\text{-}pz)_3Rh^{III}(OOH)(dppe)](BF_4)$: C. Carmona, M. P. Lamata, J. Ferrer, J. Modrego, M. Perales, F. J. Lahoz, R. Atencio, L. A. Oro, *J. Chem. Soc. Chem. Commun*. **1994**, 575.

[35] TPBN has been prepared by a method similar to that reported for TPEN: H. Toftlund, S. Yde-Andersen, *Acta Chem. Scand. Ser. A* **1981**, *35*, 575.

[36] G. Giordano, R. H. Crabtree, *Inorg. Synth.* **1990**, *28*, 88.

[37] P. T. Beurskens, G. Beurskens, W. P. Bosman, R. de Gelder, S. Garcia-Granda, R. O. Gould, R. Israel, J. M. M. Smits, DIRDIF-96. A computer program system for crystal structure determination by Patterson methods and direct methods applied to difference structure factors; Crystallography Laboratory, University of Nijmegen (The Netherlands) **1996**.

[38] P. T. Beurskens, G. Beurskens, M. Strumpel, C. E. Nordman, in *Patterson and Pattersons* (Eds.: J. P. Glusker, B. K. Patterson, M. Rossi), Clarendon, Oxford, **1987**, p. 356.

[39] A. C. T. North, D. C. Philips, F. S. Mathews, *Acta Crystallogr. Sect. A* **1968**, *24*, 351.

[40] G. M. Sheldrick, *SHELXL 97, Program for the refinement of crystal structures*, University of Göttingen, Germany, **1997**.

[41] A. L. Spek, *Acta Crystallogr. Sect. A* **1990**, *46*, C34.

[42] W. Baker, K. M. Bugg, J. F. McOmie, D. A. Watkins, *J. Chem. Soc.* **1958**, 3595.

[43] H. Brunner, B. Reiter, G. Riepl, *Chem. Ber.* **1984**, *117*, 1330.

Received: March 5, 1999 [F1650]

  0947-6539/99/0510-2936 $ 17.50+.50/0